Geological Society of America
Special Paper 409
2006

Cenozoic tectonic evolution of the eastern Rhodope massif (Bulgaria): Basement structure and kinematics of syn- to postcollisional extensional deformation

Nikolay Bonev*
Department of Geology and Paleontology, Faculty of Geology and Geography, Sofia University "St. Kliment Ohridski," BG-1504 Sofia, Bulgaria

ABSTRACT

This article contributes to a better understanding of the structure and extensional tectonics in the eastern part of the Rhodope massif. The eastern Rhodope high-grade metamorphic basement includes a lower and an upper unit of continental and mixed continental-oceanic affinity, respectively. Both high-grade basement units are tectonically overlain by a low-grade Mesozoic unit representing a Late Jurassic–Early Cretaceous subduction-accretion complex, and altogether the metamorphic units are covered by a sedimentary unit of Late Cretaceous to Miocene syn- to post-tectonic sequences. Low-angle extensional detachments and mylonitic zones separate the lower high-grade unit in the footwall from the hangingwall, consisting of the upper high-grade unit, a low-grade Mesozoic unit, greenschists, and a sedimentary unit lying in fault contact with the detachments. The high-grade basement structure consists of large-scale metamorphic domes, the Kesebir and the Byala reka domes, characterized by an overall dome-shaped regional foliation pattern and associated northwest-southeast- to northeast-southwest-trending stretching lineation. The Kesebir dome internally consists of distinct submassifs—namely, the Kesebir (s.s.), the Makaza, and the Veykata domes—distinguished from one another on the basis of structural and kinematic patterns.

Asymmetric ductile fabrics and metamorphic crystallization/deformation relationships indicate that the basement rocks experienced two distinct events of Alpine deformation: SSE-SSW–oriented contraction related to nappe stacking and top-to-the-SSW and/or -NNE extension. Top-to-the-SSE-SSW ductile fabric elements are coeval with the main metamorphism in amphibolite facies and are associated with syn-metamorphic thrust imbrication of the high-grade basement units. This contractional event occurred before intrusion of the latest Late Cretaceous–Paleocene granitoids (70–53 Ma) and is also indicated by the radiometric ages of metamorphism. The south-directed kinematics of this contractional event continued in lower metamorphic grade and temperature conditions, with top-to-the-SSW ductile to brittle extension in the Byala reka dome and top-to-the-NNE ductile rather than brittle extension in the Kesebir dome. Extension developed partly coeval and concurrent with the earlier

*E-mail: niki@gea.uni-sofia.bg.

Bonev, N., 2006, Cenozoic tectonic evolution of the eastern Rhodope massif (Bulgaria): Basement structure and kinematics of syn- to postcollisional extensional deformation, *in* Dilek, Y., and Pavlides, S., eds., Post-collisional tectonics and magmatism in the Mediterranean region and Asia: Geological Society of America Special Paper 409, p. 211–235, doi: 10.1130/2006.2409(12). For permission to copy, contact editing@geosociety.org.

stacking event through the operation of ductile to semiductile shear zones under a low-angle brittle detachment that led to tectonic denudation and exhumation of the lower high-grade unit of the footwall in the cores of large-scale metamorphic domes. The extensional exhumation was accompanied by widespread cooling of the footwall rocks in both large-scale domes between 42 and 37 Ma, followed by late faulting at 36–35 Ma. The kinematic pattern in the high-grade basement units is interpreted to reflect spatially and vertically partitioned shear sense and kinematic direction defined by stretching lineations in a metamorphic pile. This pattern formed in response to transition from crustal thickening to late orogenic extension.

The syn- to postcollisional extension described herein was broadly coeval with and followed closure of the Vardar Ocean. Extension has accommodated tectonic denudation during the late stage of the collisional evolution of the Alpine orogenic belt in the eastern Mediterranean region. The structural and kinematic results indicate that the eastern Rhodope region represents an Early–Middle Tertiary extensional domain in the northernmost part of the late Alpine Aegean extensional province.

Keywords: basement tectonics, extension, eastern Rhodope, Bulgaria

INTRODUCTION

Much insight has been gained into the process of Alpine convergence and the associated crustal shortening and thickening that resulted in nappe stacking and late orogenic extension through recent studies of the tectonics of central Rhodope, in both southern Bulgaria and northern Greece (e.g., Burg et al., 1990; Kilias and Mountrakis, 1990; Koukouvelas and Doutsos, 1990; Burg et al., 1996; Kilias et al., 1999). Recent studies of the Rhodope massif have mostly focused on the structural expression of the protracted Late Tertiary extensional tectonics (e.g., Sokoutis et al., 1993; Dinter, 1998; Kilias and Mountrakis, 1998; Wawrzenitz and Krohe, 1998; Burchfiel et al., 2003). The central Rhodope region has been interpreted as a typical metamorphic core complex of an Oligocene–Miocene age (Dinter and Royden, 1993; Dinter et al., 1995). By contrast, there is scarce information from the eastern Rhodope region about the structural style and tectonic pattern produced during the Alpine deformation episodes. Although the role of lower-crustal thrusting and detachment faulting in structural modeling and exhumation of the high-grade metamorphic rocks has recently been addressed (Bonev, 1996, 1999; Mposkos and Krohe, 2000; Bonev, 2001, 2002a,b; Krohe and Mposkos, 2002), the regional kinematics of deformation and the structural geometry of metamorphic units, especially those of the eastern Bulgarian Rhodope, in relation to crustal stacking and extension-related events remain uncertain. Therefore, the kinematics of deformation and the assessment of ductile fabrics overprinting the regional-scale structure should provide insight into the deformation style and tectonic evolution of the Rhodope massif in the extensional tectonic framework of the northernmost Aegean region.

In this article, the regional tectonic pattern of the high-grade metamorphic basement of the eastern Rhodope region in Bulgaria is examined, and kinematic evidence is provided for its complex Alpine evolution through a series of contractional and extensional deformation episodes. The aim of this contribution is therefore (1) to characterize the major structural features in the high-grade metamorphic basement and (2) to document the structures and their kinematics associated with contraction and extension-related events during the evolution of the Rhodope massif. This study is based on detailed field mapping and macro- and microscopic analysis of deformational fabric elements (particularly ductile structures) on local and regional scales, and it summarizes my own published and unpublished data as well as the structural data available in the published literature.

REGIONAL TECTONIC FRAMEWORK AND GEOLOGIC BACKGROUND

The Rhodope "massif" extends over a large part of southern Bulgaria and northeastern Greece and constitutes a major tectonic zone in the northernmost Aegean region, representing part of the Alpine-Himalayan orogenic system (Fig. 1). To the north, it is separated from the Late Cretaceous Sredna Gora volcanic arc/back-arc basin by the Alpine Maritza dextral strike-slip fault zone, and to the southwest, together with the Serbo-Macedonian massif (Ricou et al., 1998), it is limited by the Neo-Tethyan Vardar (Axios) suture zone against the internal zones of the Hellenides (Fig. 1).

The Alpine orogenic belt exposed in the Balkan Peninsula is a result of the collision between Africa and Eurasia and consists of a number of microplates that were amalgamated during the Mesozoic–Cenozoic subduction-collision history in the Tethyan realm (e.g., Dewey and Şengör, 1979; Burchfiel, 1980; Robertson and Dixon, 1984; Dercourt et al., 1986; Robertson et al., 1996). Earlier interpretations regarded the Rhodope massif as a stable Precambrian or Variscan cratonic block, unaffected by Alpine orogenic events, that was situated between

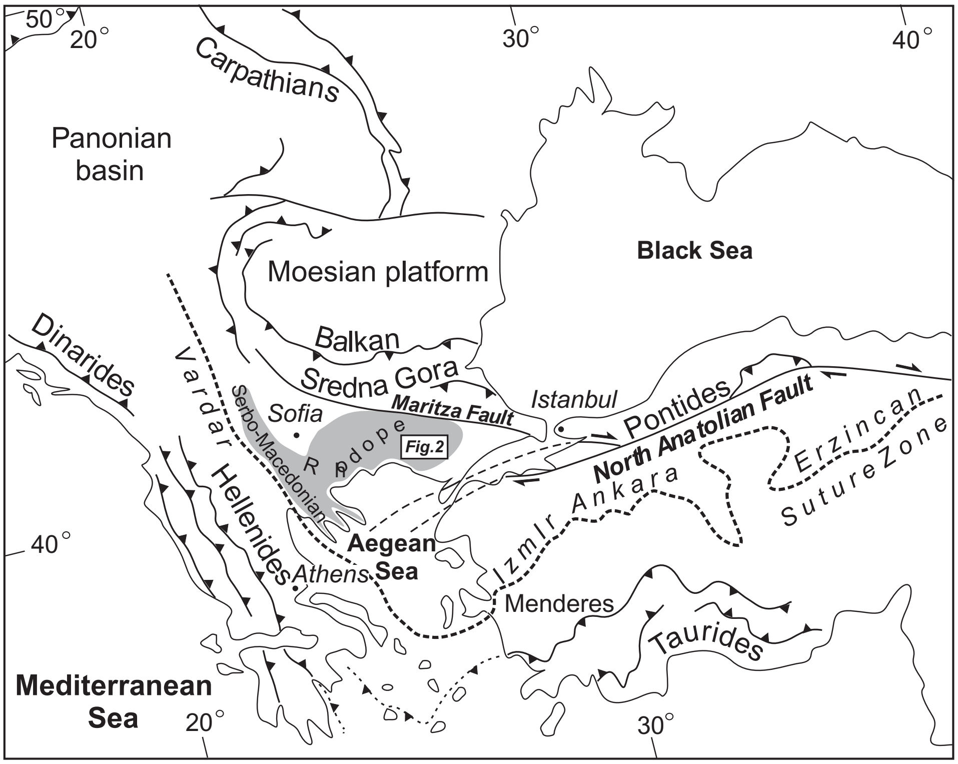

Figure 1. Sketch map showing the location of the Rhodope massif in a tectonic framework of the Alpine collisional system in the eastern Mediterranean and the study area of the eastern Rhodope. Inset: Outlines of the study area in Figure 2.

the two branches of the Alpine mountain chain, the Carpatho-Balkan belt in the north and the Dinarides-Hellenides in the south (e.g., Kober, 1928; Bonchev, 1971; Jacobshagen et al., 1978). However, the results of studies during the last two decades strongly support the interpretation of the Rhodope massif as having been actively involved in Alpine orogeny (Ivanov, 1981; Papanikolaou and Panagopoulos, 1981; Ivanov, 1988; Burg et al., 1990; Koukouvelas and Doutsos, 1990). During the Late Cretaceous–Tertiary subduction and closure of the Vardar Ocean, the collision of the continental promontory with an Adriatic-Apulian (Africa) affinity in the south with the Moesian platform (Eurasia) in the north (e.g., Robertson and Dixon, 1984; Dercourt et al., 1986) created the Rhodope massif as a crustal-scale nappe complex (Burg et al., 1996).

The Rhodope massif is dominated by a metamorphic basement comprising pre-Alpine and Alpine units of continental and oceanic affinities derived from magmatic and sedimentary protoliths. Late Cretaceous to early Miocene granitoids (Meyer 1968, 1969; Soldatos and Christofides, 1986; Del Moro et al., 1988; Peytcheva et al., 1999) intrude the basement and are covered by Late Cretaceous / Early Tertiary–Neogene volcanic and sedimentary sequences (Ivanov and Kopp, 1969; Innocenti et al., 1984; Harkovska et al., 1989; Goranov and Atanasov, 1992; Yanev and Bardintzeff, 1997; Boyanov and Goranov, 2001).

From the lithostratigraphy and metamorphic grades, it appears that the Rhodope high-grade metamorphic complex has been divided into the Pre-Rhodopian and Rhodopian Supergroups separated by an unconformity (for a review, see Kozhoukharov et al., 1988). The metamorphic sequence in the central Greek Rhodope massif has been subdivided into a lower tectonic unit (Pangeon) and an upper tectonic unit (Sidironero) separated by a major thrust fault (Papanikolaou and Panagopoulos, 1981). This subdivision was later extended into the eastern Greek Rhodope based on geological correlation of rock units and metamorphic grades (Mposkos, 1989). A regional synthesis of the Greek-Bulgarian Rhodope divided the metamorphic pile into a lower and an upper terrane sandwiching intermediate thrust sheets (Burg et al., 1996). More recently, a new subdivision into several complexes has been proposed on the basis of contrasting metamorphic histories and geochronologic data (Krohe and Mposkos, 2002). In the eastern Greek Rhodope, this subdivision interprets the Kardamos and Kechros complexes as the lowermost entities, structurally overlain by the Kimi complex along low-angle detachments (Fig. 2).

High-pressure eclogite- or granulite-facies metamorphism and later medium-pressure amphibolite-facies and late greenschist-facies metamorphism are generally recognized as the major metamorphic events in the Rhodope metamorphic complex (Liati, 1988; Mposkos, 1989; Liati and Mposkos, 1990; Mposkos and Liati, 1993; Liati and Siedel, 1996). The high-pressure metamorphism locally attained ultra-high-pressure conditions (Mposkos and Kostopoulos, 2001).

Structural overprinting relationships have been interpreted as representing separate deformation events or phases (Meyer,

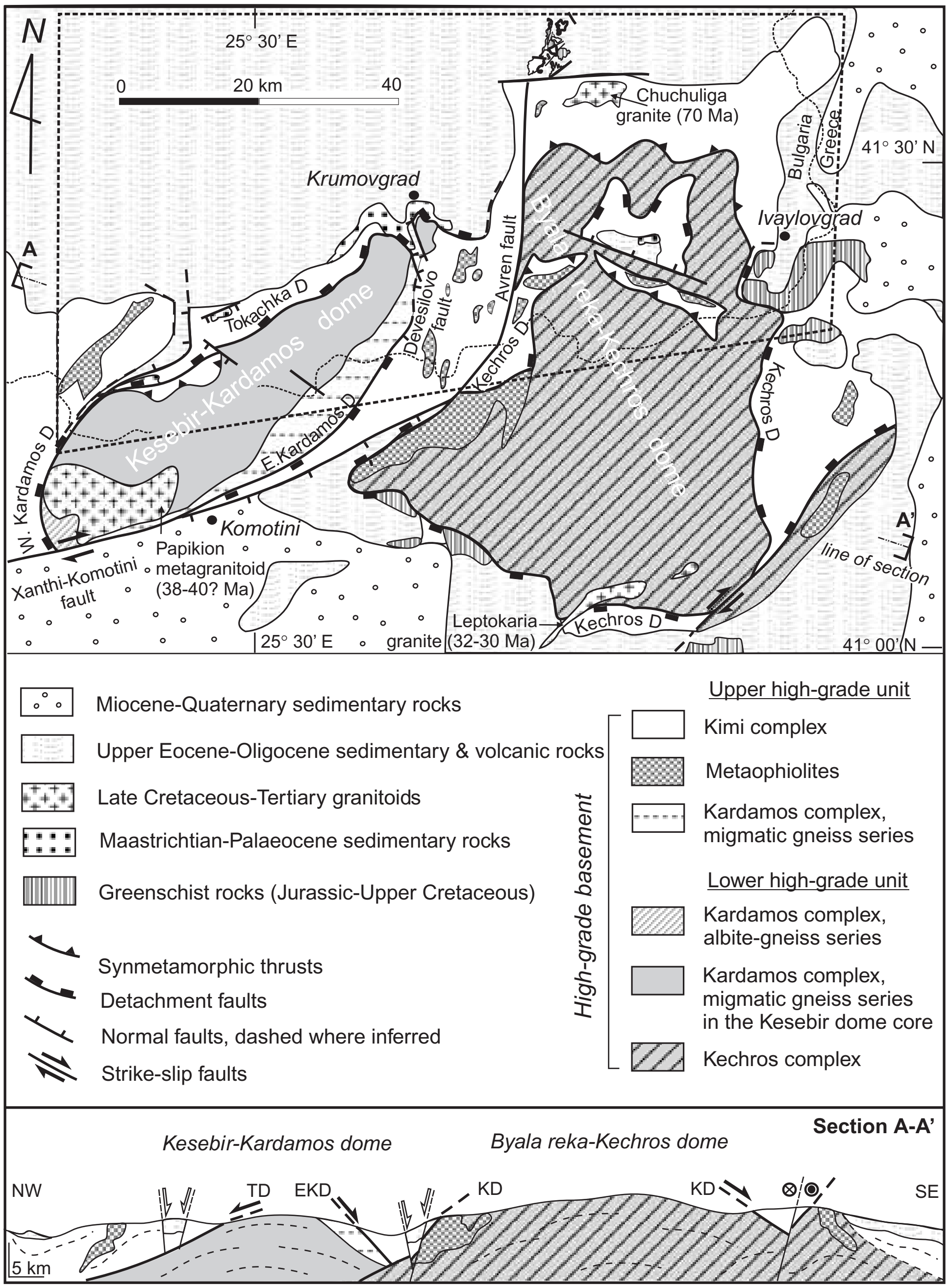

Figure 2. Synthetic tectonic map and cross-section of the eastern Rhodope showing the correlation between units, detachments, and faults across the Greece-Bulgaria border. Late granitoids broadly coeval with the crustal extension and their ages are also shown. See also Krohe and Mposkos (2002). Inset: Outlines of the study area in Figure 3. Lettering (cross-section): EKD—east Kardamos detachment; KD—Kechros detachment; M—Makaza pass; Ma—Mandrica; P—Pelevun; TD—Tokachka detachment.

1969; Papanikolaou and Panagopoulos, 1981; Ivanov et al., 1985; Barr et al., 1999) or as having been generated during a single event as part of progressive deformation broadly coeval with dominant medium-pressure-type metamorphism (Burg et al., 1990, 1996; Kilias and Mountrakis, 1990). Regionally consistent NNE-SSW-trending stretching lineations associated with the top-to-the-SSW-directed ductile fabric elements (e.g., shear structures in mylonitic gneisses) and coeval with the amphibolite-facies metamorphism were interpreted as demonstrating the transport direction during synmetamorphic nappe stacking (Burg et al., 1996). Opposite directions of tectonic transport (i.e., toward the ENE and the NNE) documented in some parts of intermediate thrust sheets were likely related to extensional deformation (Burg et al., 1996; Kilias et al., 1999). Later, Krohe and Mposkos (2002) argued that the predominantly SSW-directed shearing and kinematic patterns do not reflect progressive thrusting but are likely associated with extensional deformation.

TECTONIC UNITS OF THE EASTERN RHODOPE

The tectonostratigraphic sequence of the eastern Rhodope region, from the lowest to the highest structural levels, comprises four main units (Fig. 3; e.g., Bonev and Stampfli, 2003; Bonev et al., 2006a,b): (1) a lower high-grade unit and (2) an upper high-grade unit that both constitute the tectonic units in the high-grade metamorphic basement, (3) an overlying low-grade Mesozoic unit composed of greenschist-facies rocks, and (4) a Paleocene–Miocene sedimentary unit of cover sequences. These units are bounded by predominantly extension-related tectonic contacts and are subdivided on the base of their structural position, different lithologies and affinities, radiometric ages of protoliths, metamorphism, and the cooling or exhumation history of the rocks.

Lower High-Grade Unit

The lower high-grade unit represents the structurally deepest level in the metamorphic basement, presently exposed in windows within the cores of large-scale domal structures (Fig. 3; discussed later). The contact with the overlying upper high-grade unit is marked by extensional detachments and/or mylonitic shear zones. Lithologically, the unit represents a dominantly gneiss-migmatite series more than 6 km thick, consisting of two mica equigranular and banded orthogneisses underlain by porphyroclastic, locally porphyritic orthogneisses (metagranites) with abundant K-feldspar megacrysts. The primary intrusive relationships of both rock types are commonly obliterated by deformation and metamorphism, but magmatic textures are locally present. Based on the degree of metamorphic overprint, these rocks can be characterized as orthogneiss or metagranite, the latter showing weak recrystallization and preserved relics of magmatic flow textures (Macheva and Kolcheva, 1992; Bonev, 2002b). The orthogneisses are intercalated with migmatites and migmatitic gneisses, psammitic paragneisses, metapelites, and thin amphibolite layers at various stratigraphic levels. The lithological characteristics suggest the continental affinity of the unit, and the orthogneisses represent pre- or syndeformational granite-granodiorite intrusives hosted by sedimentary precursors of paragneisses and metapelites. The lower high-grade unit encompasses the two structurally lowest complexes defined by Krohe and Mposkos (2002) in Greece (e.g., the Kechros complex and part of the Kardamos complex; Fig. 2), and also correlates with the migmatite-orthogneiss sequence in intermediate thrust sheets of the Rhodope thrust system (Burg et al., 1996).

In the Bulgarian part, an early eclogite-facies metamorphism in metapelites at pressures of 13 kilobars and temperatures of 450 °C was followed by amphibolite-facies conditions at $P \sim 3$–9 kilobars and $T \sim 550$ °C and low-pressure, low temperature retrogressive greenschist-facies overprint at $P \sim 2 - 3$ kilobars and $T \sim 400$ °C (Macheva, 1998). In Greece, the lower unit (e.g., the Kardamos complex) records nearly isothermal decompression from maximum pressures of 13–16 kilobars for an assumed temperature of 600 °C, followed by a decrease in pressures of <8 kilobars and in temperatures of 560–620 °C during amphibolite-facies overprint in migmatized gneisses (Mposkos and Liati, 1993; Mposkos, 1998). Eclogite-facies conditions in the Kechros complex occurred at 14–15 kilobars and ~550 °C, followed by medium-pressure upper greenschist- to lower amphibolite-facies conditions at 4 kilobars (Mposkos and Liati, 1993).

Variscan protolith ages ranging between 305 and 328 Ma were obtained by U-Pb zircon and Rb-Sr whole-rock dating of lower high-grade-unit orthogneisses (Peytcheva and Quadt, 1995; Peytcheva et al., 1998). The $^{40}Ar/^{39}Ar$ mica ages of 37–38 Ma record the cooling after amphibolite-facies metamorphism that accompanied extensional exhumation of the lower high-grade unit (Bonev et al., 2006b), and the $^{40}Ar/^{39}Ar$ adularia ages of 35–36.5 Ma (Marchev et al., 2003, 2004a) document an episode of brittle extension in the hangingwall of the Tokachka and the Byala reka detachments. Similar radiometric age constraints for the lower high-grade unit were also reported in Greece for the protoliths of 334.6 ± 3.5 Ma (Mposkos and Wawrzenitz, 1995) and for the cooling or exhumation history between 36 and 42 Ma (Lips et al., 2000; Krohe and Mposkos, 2002), implying that high- and medium-pressure metamorphic events occurred prior to the Middle Eocene, or perhaps during pre–latest Cretaceous times as suggested by radiometric data for the upper high-grade unit (see also Table 1).

Upper High-Grade Unit

The upper high-grade unit represents a lithologically heterogeneous metamorphic succession composed of metasedimentary and metaigneous rocks with highly varying thicknesses (~0.1–3 km) due to tectonic omission at fault contacts. It comprises irregularly interlayered amphibolites (part of which are amphibolitized eclogites), metagabbros, metapelitic schists and gneisses (quartzofeldspathic and amphibole-bearing), marbles and calc-silicates, and rare quartzites. Small lenses and bodies of ultramafic rocks (peridotites, dunites) representing parts of a dismembered metaophiolite association (Kozhoukharova, 1984; Kolcheva and Eskenazy, 1988) occur within the unit. Petrologic studies in Greece indicate that ultramafic rocks represent a mantle association consisting of garnet-spinel lherzolites, spinel-garnet-olivine clinopyroxenites, and clinopyroxene garnetites (Mposkos, 2002). Pegmatitic and aplitic veins are particularly abundant in the succession, intruding parallel to the layering or crosscutting all rock types. The lithologic context of the upper high-grade unit together with the boninite-like chemistry of metabasic rocks suggests that the protoliths of this metamorphic sequence partially originated in a marginal basin-arc tectonic setting (Haydoutov et al., 2001; Bonev, 2002b). The upper high-grade unit is the equivalent of the Kimi complex (Krohe and Mposkos, 2002; Mposkos, 2002) in Greece (Fig. 2) and corresponds to the upper terrane of the Rhodopian nappes (Burg et al., 1996).

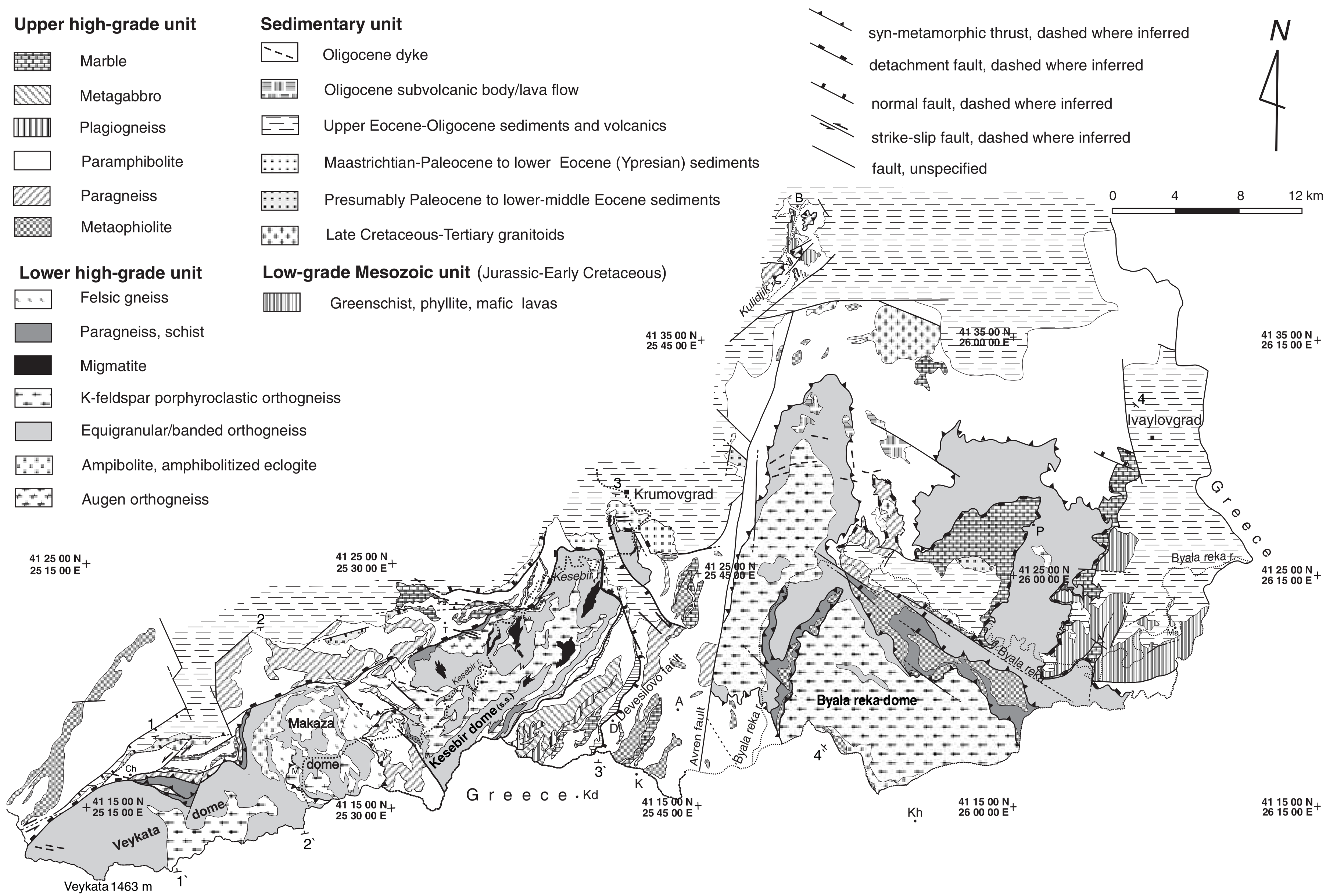

Figure 3. Simplified geological map of the Eastern Bulgarian Rhodope (compiled from Bonev, 2001, 2002a,b; Bonev and Stampfli, 2003; Bonev et al., 2006a,b; and my own unpublished data, as well as data from Goranov et al., 1995, and Dutruge, 1996). 1-1′, 2-2′, 3-3′, 4-4′: Sections of Figure 4. Lettering (villages): A—Avren; B—Bryagovets; Ch—Chakalarovo; D—Devesilovo; K—Kimi; Kd—Kardamos; Kh—Kechros; M—Makaza pass; Ma—Mandrica; P—Pelevun; T—Tokachka.

The earliest ultra-high-pressure event at pressure >26 kilobars and temperature >900 °C is documented in ultramafic rocks of the Kimi complex in Greece (Mposkos and Kostopoulos, 2001). In Bulgaria, an eclogite-facies event was estimated in the same ultramafic rocks at P ~ 12–17 kilobars and T ~ 750–811 °C, which decreased to P ~ 8–10 kilobars and T ~ 560–623 °C during medium-pressure-type metamorphism (Kozhoukharova, 1998). Lower pressure limits ~10–12 kilobars for temperatures of 440–520 °C were obtained for a retrograde metamorphic path to amphibolite and greenschist facies of an eclogite (Mukasa et al., 2003). Similarly, the high-pressure, high-temperature eclogite- or granulite-facies conditions in the Kimi complex at P ~ 13.5–16 kilobars and T ~ 750–775 °C decreased to ~10 kbar and 600–650 °C during a medium-pressure event, then subsequently retrogressed into the greenschist facies (Mposkos and Krohe, 2000; Mposkos, 2002).

U-Pb ion microprobe dating of zircon domains in gabbro yielded a Neoproterozoic protolith with an age of 572 ± 5 Ma in the core, and the rims yielded Variscan metamorphic ages of ca. 300–350 Ma (Carrigan et al., 2003). A Sm-Nd garnet-clinopyroxene whole-rock age of 119.6 ± 3.5 Ma from garnet-spinel pyroxenite (Wawrzenitz and Mposkos, 1997) and a U-Pb sensitive high-resolution ion microprobe age obtained from zircon domains (e.g., core) in another garnet-rich mafic rock of 117.4 ± 1.9 Ma (Liati et al., 2002) were interpreted by the former authors as the age of the high-pressure metamorphism or as the age of crystallization of the protolith by the latter authors. The possibility that these ages may record an early stage of exhumation of the ultra-high-pressure event is not excluded by either set of authors (from depth 200–60 km at P ~ 16 kilobars and T ~ 800 °C; e.g., Mposkos, 2002). Nevertheless, these two similar radiometric ages point to the strong imprint of an Early Cretaceous tectonometamorphic event. The zircon domains (e.g., rims) in the same garnet-rich mafic rocks also yielded an age of 73.5 ± 3.5 Ma for the high-pressure, eclogite-facies metamorphism and an age of 61.9 ± 1.9 Ma for the late retrogressive stage (Liati et al., 2002). The Rb-Sr whole-rock age of 65.4 ± 0.7 Ma from an undeformed pegmatite is interpreted to date the amphibolite-facies metamorphism and to provide a minimum age for the migmatization (Mposkos and Wawrzenitz, 1995). Syn- to post-tectonic granites that occur intrusive into the upper high-grade unit (Chuchuliga granite, Fig. 2) were dated at ca. 70 Ma by a U-Pb zircon method (Marchev et al., 2004b). The $^{40}Ar/^{39}Ar$ amphibole and muscovite ages, respectively, of 45 ± 2 Ma and 39 ± 1 Ma (Mukasa et al., 2003) bracket the cooling history from amphibolite- to greenschist-facies conditions.

Low-Grade Mesozoic Unit

The low-grade Mesozoic rocks (Jaranov, 1960; Boyanov and Russeva, 1989) are unique to the eastern Rhodope tectonostratigraphic unit, lying tectonically on the high-grade metamorphic basement. These weakly metamorphosed rocks are conventionally regarded as representing extension into the eastern Rhodope of the circum-Rhodope belt, which surrounds the Serbo-Macedonian massif in the south (see Fig. 1; e.g., Kauffmann et al., 1976; Kockel et al., 1977; Papanikolau, 1997). The fossil evidence yielded mostly Early–Middle Jurassic to Early Cretaceous stratigraphic ages (Trikkalinos, 1955; Tikhomirova et al., 1988; Dimadis and Nikolov, 1997), and K/Ar hornblende and the apatite fission-track ages of magmatic rocks range between ca. 140 and 161 Ma (Biggazzi et al., 1989; Tsikouras et al., 1990). These stratigraphic and radiometric ages suggest that the greenschist-facies metamorphism of the low-grade Mesozoic unit took place significantly before the similar-grade metamorphism in structurally deeper high-grade basement units. In Bulgaria, the low-grade Mesozoic unit consists of greenschist (chlorite and actinolite are common) and phyllite at the base, overlain by tholeiitic basic-intermediate lava flows and metapyroclastic rocks. These grade upsection into a terrigenous-marly turbiditelike succession of conglomerate, sandstone, and phyllitic shale enclosing reworked clastics of deep-water sediments, Late Permian and Middle–Late Triassic shallow-water carbonates, mafic rocks, and greenschist. The Campanian tuffaceous strata found at the uppermost level of the low-grade Mesozoic unit depositionally overlies lithologies of the latter and the high-grade basement units (Boyanov and Russeva, 1989). The metamorphic grade decreases upward from a locally epidote-amphibolite, dominantly greenschist-facies condition to very low-grade metamorphic conditions. Recently, based on our structural data and the chemistry of greenschist rocks and mafic lavas, we interpreted the Mesozoic unit as a Late Jurassic–Early Cretaceous island arc accretionary assemblage in the Tethyan domain (Bonev and Stampfli, 2003).

Sedimentary Unit

At the top of the tectonostratigraphic section, a supracrustal sedimentary unit of cover sequences ranging in age from the Late Cretaceous to the Miocene (see Boyanov and Goranov, 2001, for a review) represents syn- and post-tectonic deposits accumulated in fault-bounded, small half-grabens. These cover sequences prograde toward the large sedimentary basin, the east Rhodope depression, in the north, or rest unconformably on the low- and high-grade metamorphic units. The sedimentary unit consists, in ascending order, of Maastrichtian–Paleocene to lower Eocene (Ypresian) coarse clastic colluvial-proluvial sedimentary rocks of the Krumovgrad Group (Goranov and Atanasov, 1992). These deposits form part of the hangingwall suite accumulated in supradetachment half-grabens (Figs. 3 and 4; Bonev, 2002b) and consist of boulder breccias, olistoliths, and breccia-conglomerates derived only from the upper high-grade unit. The Krumovgrad Group is unconformably overlain by upper Eocene (Priabonian)–Oligocene sedimentary rocks observed in three suites: breccia-conglomerate, coal-bearing sandstone, and marl-limestone formation. These formations collectively mark a renewed transgressive cycle of terrigenous continental fresh-water to marine sedimentation that was ac-

TABLE 1. SUMMARY OF FABRICS, METAMORPHISM, AND TIMING OF DEFORMATIONAL EVENTS IN THE HIGH-GRADE METAMORPHIC BASEMENT

Tectonic setting	Fabrics	Textures	Deformation	Metamorphic conditions	Units / rock type / regional structure	Age (Ma)*	References
Subduction	Earliest (?) ultra-high-pressure relics preserved in lenses of retrogressed eclogites and metapelites	Multicrystalline polygonal quartz aggregates and diamond inclusions, exsolution of quartz rods (coesite) and rutile needles in garnet	Deep crustal-level underthrusting	Ultra-high-pressure metamorphism $P > 26$ kbar and $T > 900$ °C (possibly 40–70 kbar and $T > 1000$ °C), based on mineralogical criteria	Upper high-grade unit (Kimi complex, Greece) metapelite, garnet-biotite-kyanite gneiss, SE flank the Kesebir-Kardamos dome, near Kimi village	N.D.†	Mposkos and Kostopoulos (2001)
					Upper high-grade unit (Kimi complex, Greece) garnet-rich mafic rock, magmatic crystallization of mafic protolith	117.4 ± 1.9	Liati et al. (2002)
	Layering in metaperidotite	Porphyroclastic, granoblastic		High-pressure / high-temperature (eclogite/ granulite facies), $P > 13.5$–16 kbar, $T = 750$–775 °C	Upper high-grade unit (Kimi complex, Greece) garnet-pyroxenite (metagabbro) with assemblage hornblende-spinel-olivine-garnet-clinopyroxene, SE flank of the Kesebir-Kardamos dome, near Kimi village	119.6 ± 3.5	Wawrzenitz and Mposkos (1997)
		Lens-shaped		$P > 12$–17 kbar, $T = 750$–811 °C	Upper high-grade unit (Bulgaria) amphibolized eclogite SE flank of the Kesebir-Kardamos dome, near Avren village		Kozhoukharova (1998)
Collision / crustal thickening				Eclogite facies	Upper high-grade unit (Kimi complex, Greece) garnet-rich mafic rock	73.5±3.5	Liati et al. (2002)
		Porphyroblastic	Early mylonitic deformation, contractional SSE–SSW-directed ductile syn-metamorphic thrusting and nappe stacking of the high-grade units	P 13-16 kbar, T ~600 °C	Lower high-grade unit (Kimi complex, Greece) Metapelite, gneiss		Mposkos and Liati (1993)
				P 13 kbar, T 450 °C	Metapelite, Byala reka dome		Macheva (1998)

	Main foliation development, e.g., regional foliation (S1) and mineral lineation (L1), tight to isoclinal small-scale rafolial folds	Protomylonitic tomylonitic, porphyroblastic common growth of synkinematic garnet, kyanite, and staurolite porphyroblasts		Medium-pressure amphibolite facies $P > 10$ kbar, $T = 600–650$ °C	Upper high-grade unit (Kimi complex, Greece)		
					Metapelite		Mposkos and Krohe (2000) (1995)
					Undeformed pegmatite	65.4 ± 0.7	Mposkos and Wawrzenitz (1995)
					Undeformed pegmatite	61.9 ± 1.9	Liati et al. (2002)
				$P \sim 10–12$ kbar, $T = 440–520$ °C	Upper high-grade unit (Bulgaria) retro-gressed eclogite, Byala reka dome	45 ± 2 –39 ± 1	Mukasa et al. (2003)
				$P < 8$ kbar, $T = 560–620$ °C	Lower high-grade unit metapelite, Byala reka dome (Greece)		Mposkos and Liati (1993)
				P 3–9 kbar, $T \sim 550$ °C	Lower high-grade unit metapelite, Byala reka dome (Bulgaria)		Macheva (1998)
Inception of extension	Weak foliation at the contacts	Nonpenetrative	Intrusive, cross-cutting regional foliation (S1)	Shallow-level granitic bodies	Upper high-grade unit (Bulgaria) leucocratic granite, Byala reka dome (e.g., Fig. 2)	69 ± 1	Marchev et al. (2004b)
					Central eastern Rhodope (Bulgaria)	52.89 ± 0.89	Ovtcharova et al. (2003)
Extension, exhumation, and doming		Mylonitic, chlorite growth after synkinematic porphyroblasts	Ductile to semi-ductile extensional shear zones, mylonitic foliation (Sm) and stretching lineation, crenulation cleavage (S2), low-angle detachments	Amphibolite to greenschist facies, $P \sim 3$ kbar, $T \sim 400$ °C	Byala reka dome (Bulgaria) metapelite		Macheva (1998)
				Cooling of high-grade basement rocks after amphibolite facies in the footwall of the detachments	Byala reka dome (Greece)	42–36	Lips et al. (2000)
					Kesebir dome (Greece)	42–39	Krohe and Mposkos (2002)
					Kesebir dome (Bulgaria)	38–37	Bonev et al. (2006a)
		Cataclastic, microbreccia, gouge	Upper crustal brittle extension, NE-SW and NW-SE-trending fault sets	$T < 200$ °C	Hydrothermal alteration along faults in supra-detachment sedi-mentary deposits		
					Byala reka dome (Bulgaria)	36.5	Marchev et al. (2003)
					Kesebir dome (Bulgaria)	35	Marchev et al. (2004a)

Notes:
*Methods and minerals are given in the text.
†N.D.—Not determined.

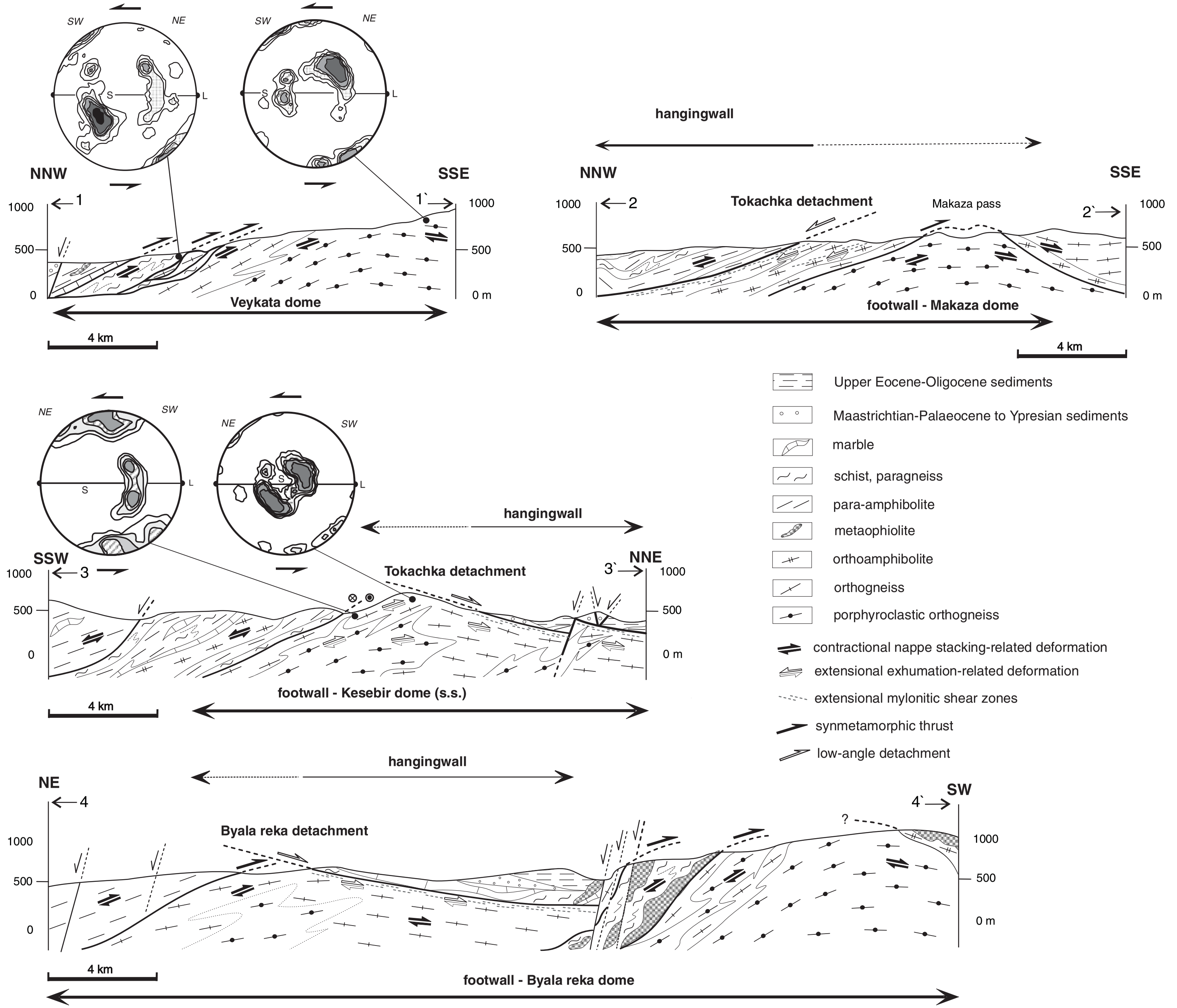

Figure 4. Synthetic cross-sections of the metamorphic domes located in Figure 3 and showing the dome structural geometries and kinematics with elements of the detachment fault system. Quartz *c*-axis fabric with deduced shear sense is indicated for the respective locations, 240 *c*-axis per diagram, contours 1–6%.

companied by voluminous late Eocene–Oligocene volcanic rocks and sedimentary-volcanogenic successions. The breccia-conglomerate formation has been suggested to be of an early Eocene age (e.g., Boyanov and Goranov, 2001), yet the fossil evidence is lacking. The Miocene–Pliocene alluvial-proluvial deposits represent a new transgressive cycle onto the crystalline basement and the Paleogene successions and are widespread in the northeasternmost part of the eastern Rhodope region.

LARGE-SCALE BASEMENT STRUCTURES, FAULTS, AND SHEAR ZONES OF EXTENSIONAL PATTERN

General

In this section a brief description of the basement structure and the most important displacement zones of the extensional pattern is given. The main focus is on outlining the spatial and temporal relationships of the high-grade metamorphic units and the major faults and shear zones involved in extensional exhumation of the metamorphic domes.

The high-grade basement in eastern Rhodope was described as consisting of large-scale folds with an assumed pre-Variscan or Precambrian age (Ivanov, 1961; Boyanov et al., 1963; Boyanov and Kozhoukharov, 1968; Kozhoukharov, 1971, Kozhoukharov et al., 1988). However, neither radiometric ages nor regional constraints on tectonostratigraphy allow us to support this tectonic interpretation. Instead, the large-scale tectonic pattern is defined by metamorphic domes exposed in the footwall of presently low-dipping detachment faults. On a regional scale, two large-scale, late Alpine metamorphic domes, namely the Kesebir and the Byala reka domes, from west to the east, dominate the structural shape and the topographic pattern that continue into northern Greece (Fig. 3). The Kesebir dome was earlier named the Kesebir-Kardamos dome (Bonev et al., 2006b), and the Byala reka dome was correspondingly designated the Byala reka–Kechros dome based on regional correlations (Bonev et al., 2006a; Fig. 2). Both structural domes are outlined by a pattern of regional foliation in the high-grade basement-unit rocks. The lower high-grade unit is presently exposed in tectonic windows below low-angle detachment surfaces within the cores of the domes flanked by the structurally overlying upper high-grade unit. The foliation typically wraps around the gneissic cores and dips outward to delineate the large-scale dome-shaped metamorphic culminations (Figs. 4 and 5).

Kesebir Dome

The Kesebir dome is a northeast-trending metamorphic dome exposed in the high-grade basement from the Greek-Bulgarian boundary in the southwest to the town of Krumovgrad to the northeast (Bonev, 2002b; Bonev et al., 2006b). Based on kinematic patterns and structural and outcrop map features, the Kesebir dome has been internally subdivided into the Kesebir dome (s.s.), which coincides with the larger metamorphic massif centered along the Kesebir River Valley, and two separate, smaller submassifs (the Makaza dome and the Veykata dome) occupying the southwestern end of the large-scale Kesebir-Kardamos dome (Figs. 2 and 3).

The Kesebir dome (s.s.) is a structural dome occupying an area of 20 × 20 km, whose nearly subhorizontal axis with an average direction N 046 (stereoplot *h,* Fig. 5) parallels the Kesebir River Valley. The dome is cored by medium-pressure amphibolite-facies orthogneisses and migmatites of the lower high-grade unit and mantled by a lithologically heterogeneous upper high-grade unit. Sillimanite-bearing migmatites in the core indicate a late, high-temperature amphibolite-facies overprint during decompression (Bonev, 2004). The Makaza dome exposes similar lithologic associations of both high-grade metamorphic units. The lower unit consists of a relatively thick discontinuous amphibolite horizon (not present in the Kesebir dome [s.s.]) mirroring orthogneisses from below, thus defining a nearly radial structural pattern (stereoplot *e,* Fig. 5) of an ~10 × 10 km metamorphic dome centered at the Makaza Pass. Farther southwest, the Veykata dome is a half-window that straddles the Greek-Bulgarian boundary, closing in the south in Greece. It is represented by its northeastern closure, whose axis gently plunges (N 62/25) ENE (stereoplot *c,* Fig. 5). A thick (>5 km), monotonous orthogneiss of the lower high-grade unit is exposed within the core, flanked by the upper high-grade unit to the north-northwest. The anatexis phenomena are not well developed within the cores of both latter domes, contrary to the situation in the Kesebir dome (s.s.). Subsolidus melt mobilization occurs as aplitic-pegmatitic veins, but typical migmatites and anatectic granites are lacking.

A low-angle normal fault, the Tokachka detachment (Bonev, 1996), bounds the large-scale Kesebir dome to the north. Both high-grade units on the north-northwestern flank of the dome are juxtaposed against the detachment surface, which is in turn underlain by mylonites comprising a normal dip-slip top-to-the-NNE ductile shear zone. This shear zone evolved in decreasing metamorphic grade from amphibolite to greenschist facies, initially defining a break in the metamorphic grade, then later marking the ductile to brittle transition across the contact toward the detachment (Bonev et al., 2006b). At the latitude of the Veykata dome, the NNW-dipping detachment surface truncates a ductile mylonite zone showing top-to-the-SSE to SSW shearing in amphibolite facies (Bonev, 2001) at the northern flank of the structure, and it bounds the Makaza dome farther northeast. In northern Greece, the western Kardamos detachment of Krohe and Mposkos (2002) seems to represent a counterpart of the detachment bounding the Kesebir dome. The structural boundary between basement units on the opposite, southeast-dipping flank of the Kesebir dome (s.s.) is marked by a mylonitic shear zone that shows no break in the metamorphic grade. This shear zone shows a top-to-the-south-SSW ductile fabric and has been interpreted as a reactivated pre-extension but syn-metamorphic contact. Farther southeast, the moderately ESE-dipping Devesilovo fault cuts through the upper high-grade unit,

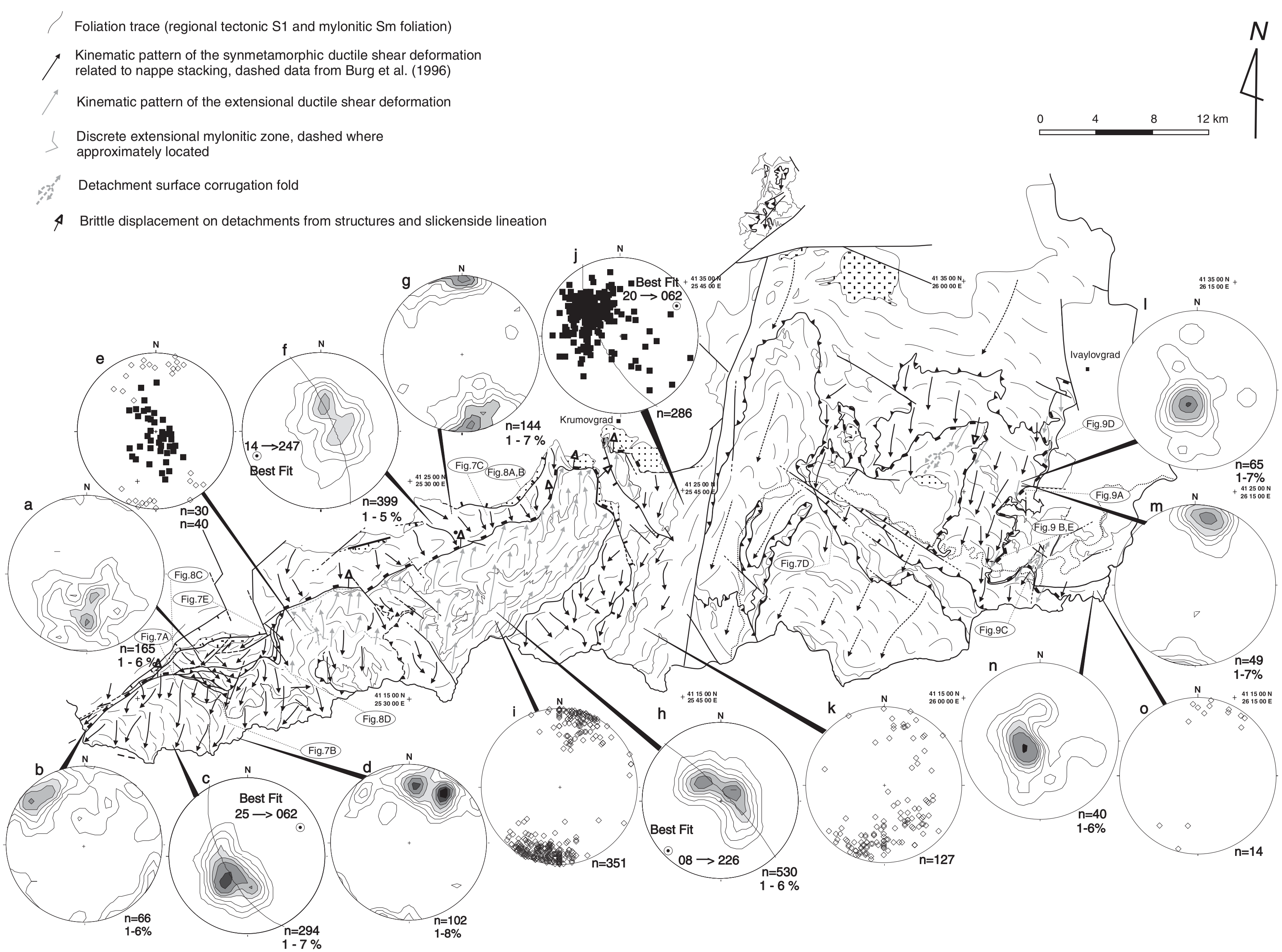

Figure 5. Structural map and kinematic pattern of the metamorphic basement in the eastern Rhodope. The arrows point to the displacement of tectonic top with averaged direction from several lineation measurements associated with locally systematic shear sense. The black arrows point to the sense of shear on inferred thrust movement, whereas the gray arrows point in the direction of shear associated with extensional deformation. Stereoplots (lower hemisphere, equal area projection): *a–b,* foliation and lineation, respectively, in the mantle of the Veykata dome; *c–d,* foliation and lineation, respectively, in core of the Veykata dome; *e,* foliation (squares) and lineation (rhombs) in the Makaza dome; *f–g,* foliation and lineation, respectively, in the mantle of the Kesebir (s.s.) dome; *h–i,* foliation and lineation, respectively, in the core of the Kesebir (s.s.) dome; *j–k,* foliation and lineation, respectively, in the mantle of the Kesebir (s.s.) dome; *l–m* and *n–o,* foliation and lineation, respectively, in the central–eastern Byala reka dome.

facilitating the unroofing of separate levels of the latter, as portrayed by different metamorphic sections exposed on both sides of the fault. This normal fault most likely represents an extension of the eastern Kardamos detachment surface of Mposkos and Krohe (2000).

The detachment surface bounding the northern side of the large-scale Kesebir dome has controlled hangingwall sedimentation in the supradetachment basin, which occurs generally parallel to its map trace and the dome elongation direction. The basin fill starts at the bottom with the basal Maastrichtian–Paleocene to early Eocene deposits of the Krumovgrad Group (Goranov and Atanasov, 1992) resting directly on the fault contact of the Tokachka detachment surface. These rocks are in turn overlapped by upper Eocene–Oligocene deposits of the cover sequences. At the northern closure of the Kesebir dome (s.s.), the latter sediments fill the superimposed small fault-bounded northwest-southeast-oriented graben, in which the strata progressively thicken and young toward the steeply southwest-dipping, graben-bounding normal fault to the northeast. Small fault-bounded half-grabens, filled with undated coarse breccias similar to those of the Krumovgrad Group, also occur north of the Makaza dome. To the north of the Veykata dome, the hangingwall deposits at the base of the supradetachment basin comprise analogous clastic sediments. These sedimentary deposits in the last two occurrences are attributed to the lower Paleogene Krumovgrad Group (Boyanov and Goranov, 2001). Therefore, they represent the sedimentary fill of extension-related and fault-bounded grabens developed on the upper high-grade unit of the hangingwall.

Byala Reka Dome

The Byala reka dome is a north-trending structural dome located east of the Kesebir dome and exposed in the Byala reka River Valley in the easternmost part of the Rhodope massif (Fig. 3). This flat, wide metamorphic dome (40 × 40 km) exhibits coherent lithologic associations of both tectonic units in the high-grade metamorphic basement (stereoplot *l,* Figs. 4 and 5) below the structurally overlying low-grade Mesozoic unit. The metamorphic section of the lower high-grade unit, compared to the Kesebir dome, is characterized by the presence of large slivers of metaophiolitic rocks, which are widespread in the upper high-grade unit. These meta-ophiolites are generally confined by synmetamorphic thrust contacts (e.g., Burg et al., 1996) at the northern Byala reka dome. There are no typical migmatites in the lower high-grade unit, suggesting that partial melting processes did not take place during its evolution.

In the central Byala reka dome, the two high-grade tectonic units are separated by a brittle tectonic contact known as the Pelevun thrust (Ivanov, 1961; Boyanov et al., 1963). This thrust fault separates a thin lid, made of marbles with subordinate gneisses and schists of the upper high-grade unit, from underlying orthogneisses of the lower high-grade unit. Reconnaissance observations at this contact suggest, however, that this structure defines a detachment or décollement with footwall mylonites showing SSW-directed shearing (Bonev et al., 2006a). The eastern flank of the dome is marked by an east-southeast-dipping, low-angle extensional shear zone between both high-grade metamorphic units below the structurally overlying low-grade Mesozoic unit (Bonev and Stampfli, 2003). This mylonitic zone was interpreted as a detachment or décollement surface placing a strongly thinned upper high-grade unit on top of the lower-unit mylonites of the footwall. Collectively, the central and eastern occurrences of the detachment in the Byala reka dome represent a regional fault surface, which is hereafter referred to as the Byala reka detachment. The structural boundary between two high-grade units outcropping in the Byala reka dome was identified as the Kechros detachment, bounding the dome on both flanks in Greece (Fig. 2; Krohe and Mposkos, 2002). To the west, the Byala reka dome is limited by a steep fault known as the Avren dislocation that accommodated normal displacement during the Paleogene (Ivanov, 1961). Recently gathered seismic data have shown that the Avren fault is a deeply seated prominent crustal structure with numerous synthetic second-order splays uplifting ductile-brittle transition and "Moho" boundaries to depths of between 10 and 30 km (Velev, 1996), respectively. Therefore, the Avren fault confining the western flank of the Byala reka dome defines the structural boundary with the Kesebir dome westward.

A fault-bounded northwest-southeast-oriented half-graben has developed on the marble lid of the upper high-grade unit, filled by coarse clastic Paleocene–middle Eocene deposits (breccia-conglomerate formation, Krumovgrad Group) and upper Eocene–Oligocene fresh-water to shallow-marine sediments (sandstone-coal-bearing formation; e.g., Boyanov and Goranov, 2001). Within the half-graben, basal breccias and breccia-conglomerates that include clasts derived from the low-grade Mesozoic unit and sandstone strata are tilted south-southwest toward a steeply northeast-dipping normal fault bounding the southwestern side of the half-graben. To the north and east, the high-grade units in the Byala reka dome are unconformably covered by the upper Eocene–Oligocene sedimentary formations, volcanics, and volcanogenic-sedimentary rocks.

Geometrically and kinematically, the Byala reka dome differs from the Kesebir dome, showing a tectonic transport direction toward the south-southwest that has been related either to synmetamorphic thrusting (Burg et al., 1996) or to an extensional detachment faulting (Krohe and Mposkos, 2002).

DEFORMATION PATTERN AND KINEMATICS

Field observations and microstructural analysis were combined to determine the ductile fabrics formed during different deformation events, with their kinematics and relative timing deduced from relationships between metamorphic crystallizations and deformational fabrics. Metamorphic rocks consisting of high-grade basement units have experienced two geometrically and kinematically distinct deformation events or phases of

Alpine deformation—top-to-the-SSE-SSW contraction and top-to-the-SSW and top-to-the-NNE extension. Kinematic observations have been made in outcrops and thin sections oriented parallel to the lineation (*x*-axis) and perpendicular to the foliation (*xy*-plane). The following section focuses on the synthesis of deformation and the kinematics of high-grade basement rocks (see Table 1), in particular amphibolite to greenschist-facies mylonites, and covers the whole Kesebir dome and central–eastern part of the Byala reka dome.

Top-to-the-SSE-SSW Contractional Fabrics

The earlier penetrative ductile deformation is characterized by a regional tectonic foliation (S_1) and the associated mineral elongation and/or stretching lineation (L_1). The foliation in the lower high-grade unit is gneissic foliation or schistosity defined by oriented micas, flattened feldspars, and quartz ribbons or represents gneiss banding and migmatitic layering. In the upper high-grade unit, the foliation is marked by a compositional layering delineated by a fine alternation of thin layers of distinct lithologies or ubiquitous schistosity. The foliation is commonly associated with a mineral lineation defined by a preferred orientation of elongated quartz, feldspar, white mica, biotite, amphibole, and mineral fringes on garnet, staurolite, and kyanite porphyroblasts. The regional distribution of both the regional tectonic foliation (S_1) and the mineral stretching lineation (L_1) varies across the study area. The foliation trajectories form patterns that are subelliptical (e.g., the Kesebir [s.s.] and Veykata domes), radial (e.g., Makaza dome), or concentric (e.g., Byala reka dome) in the lower high-grade unit within the cores of distinct domes and are associated with a generally northeast-southwest-trending stretching lineation (Fig. 5). In the upper high-grade unit, all along the northwestern flank of the Kesebir dome the foliation strikes northeast-southwest to east-west, dips moderately to the northwest, the southeast, or north-south (stereoplots *a* and *f,* Fig. 5), and contains a lineation consistently oriented northwest-southeast, plunging in both directions (stereoplots *b* and *g,* Fig. 5). The southeastern flank of the dome exhibits a foliation that homoclinally dips southeast, bearing a northwest-southeast- to northeast-southwest-trending lineation from deepest to shallow structural levels, respectively (stereoplots *j* and *k,* Fig. 5).

In the core of the Veykata dome, the moderately NNE-dipping foliation is associated with a predominantly shallow, NNE-plunging lineation (stereoplots *c* and *d,* Fig. 5). The Makaza dome presents NNW-SSE to north-south lineation trends on a gently dipping foliation (stereoplot *e,* Fig. 5). In the Byala reka dome, the flat-lying foliation contains a subhorizontal to shallow northeast- or southwest-plunging lineation (stereoplots *l–o,* Fig. 5).

Mesoscopic, asymmetric tight to closed or subisoclinal folds have axes parallel to the mineral lineation in the Veykata dome, in the upper high-grade unit on the flanks of the Kesebir dome (s.s) and Byala reka dome (Fig. 6), showing predominantly south-southwest vergence. Asymmetric macro- and microstructures used as shear sense criteria, such as asymmetric boudinage, C/S fabrics, shear band cleavage, oblique grain-shape foliation, and quartz *c*-axes' preferred orientation, are abundant in the rocks (Figs. 4 and 7). Shear sense indicators in the upper high-grade unit show regionally consistent top-to-the-SSE tectonic transport on the flanks of the Kesebir dome, top-to-the-SSW shear sense in the core of the Veykata dome, top-to-the-SSE shear sense on the southern flank and at the crest of the Makaza dome, and top-to-the-southwest shear sense in both high-grade units in the Byala reka dome (Fig. 5).

The relationships between metamorphic crystallizations and ductile fabrics are best preserved in metapelites and amphibolites in the upper high-grade unit as well as in the lower high-grade unit orthogneisses. Syntectonic porphyroblasts in the metamorphic assemblage have crystallized during ductile deformation and associated top-to-the-SSE-SSW shearing. Garnet porphyroblasts exhibit pronounced synkinematic growth traced by abundant hellicitic inclusion trails of amphibole and quartz, or developed white mica, biotite, kyanite, and staurolite crystal-

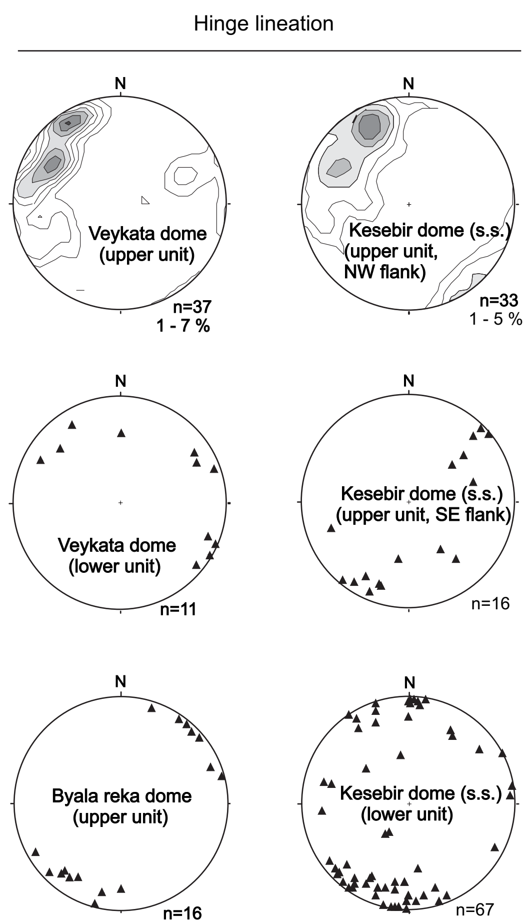

Figure 6. Summary of orientational data of small-scale folds in the high-grade basement across the study area. Lower hemisphere, equal area projections.

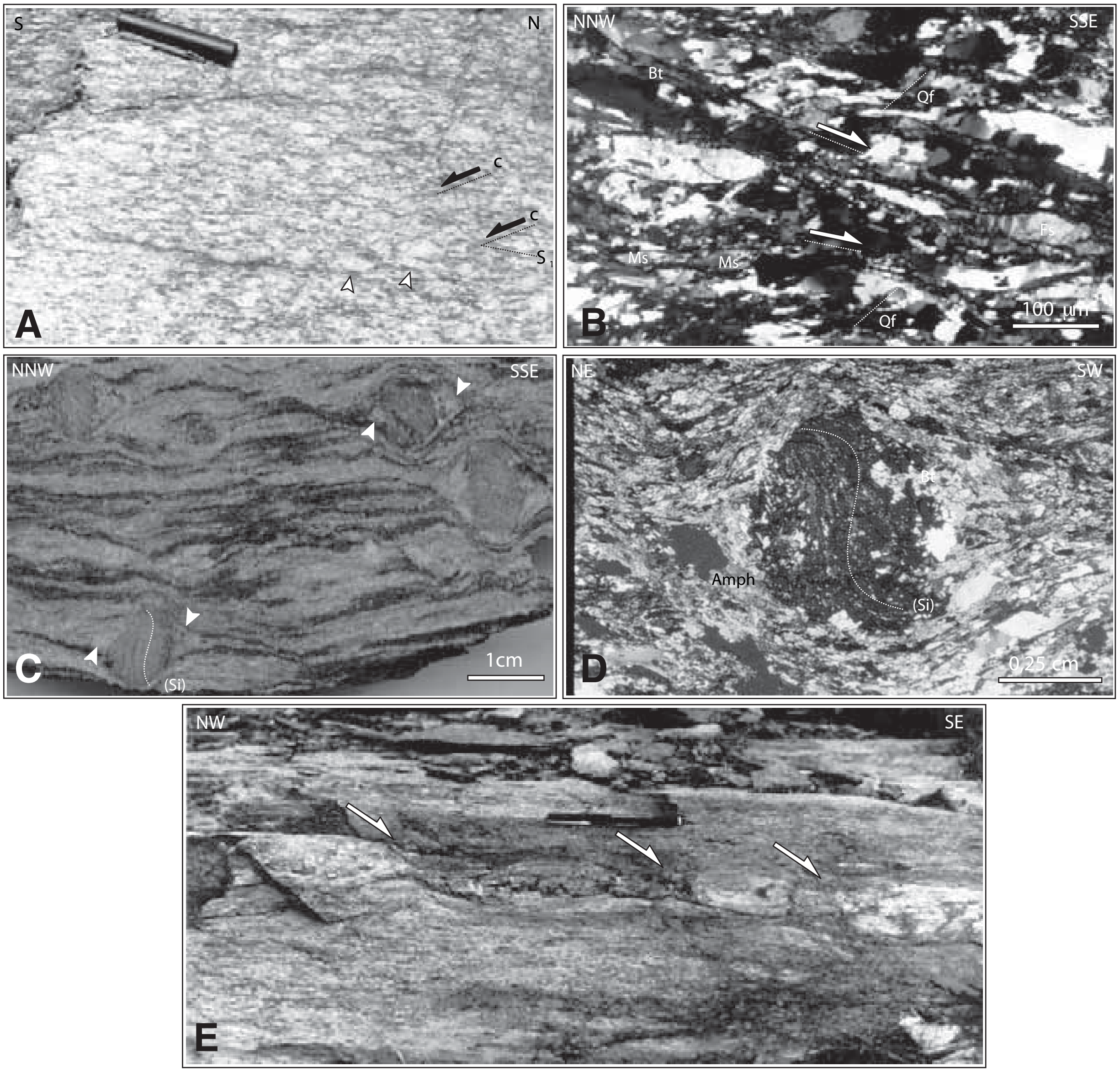

Figure 7. Ductile fabrics and shear criteria associated with the top-to-the-SSE-SSW tectonic transport related to synmetamorphic nappe stacking. (A) C/S fabrics (black half-arrows) and σ-type clasts (white arrows) in K-feldspar porphyroclastic orthogneiss. (B) C′ shear bands (white half-arrows), mica fiches (Ms), and grain-shape oblique foliation in quartz ribbons (Qf) in mylonitic gneiss. Bt—biotite. (C and D) Garnet porphyroblasts with asymmetric pressure shadows (arrows) and sigmoidal-shaped inclusion trails pattern defining internal foliation (Si). Amph—amphibole. (E) Asymmetric boudinage of aplitic gneiss in garnet-rich metapelite. Shear sense indicated; for locations, see Figure 5.

lizations in asymmetric pressure shadows consistent with bulk southward shear sense (Fig. 7C and D). These relationships imply coeval metamorphic growth and south-directed ductile shear during the main medium-pressure-type metamorphism in amphibolite-facies conditions.

Synmetamorphic, ductile mylonite zones depicting contractional fabrics have accommodated thrust displacement during crustal stacking or imbrication of separate levels of both high-grade units. In the Byala reka dome, the main mylonitic zone sandwiching metaophiolite slices between lower-unit orthogneisses occur at the dome crest, as well as along a distinct thrust contact juxtaposing lower and upper high-grade units at the northern closure of the dome (Figs. 3 and 4; cf. Burg et al., 1996; Bonev et al., 2006a, their Fig. 4; and this study). At the latitude of the Veykata dome, the mylonitic thrust zone on the northern flank consists of thin slices of imbricated gneisses from the lower high-grade unit and is associated with down-dip foliation and lineation and top-to-the-SSW up-dip synmetamorphic ductile shear (section 1-1′, Fig. 4; Bonev, 2001). On the southern flank of the Makaza dome, the S-dipping mylonite zone also accommodates S-directed thrust displacement, whereas those on the eastern flank of the dome may have been modified by subsequent deformation or may reflect more distributed shear deformation. It is important to note that the former mylonite zone imbricates slices of mafic rocks between the lower-unit orthogneisses, whereas the latter places mafic-ultramafic rocks (peridotite, metagabbro) on top of them. Another important thrust displacement zone, the so-called Kulidjik nappe (Boyanov, 1969), occurs on top of the low-grade Mesozoic unit along the Kulidjik River Valley north of the Byala reka dome (see location lettered B, Fig. 3). Preliminary kinematic analysis at the base of the hangingwall of this thrust shows top-to-the-SSW displacement of the allochthonous muscovite gneisses from the upper high-grade unit that post-dates pervasive alteration of the underlying Mesozoic greenschists (Bonev, 2006).

Top-to-the-NNE Extensional Fabrics

It has been shown that the earlier synmetamorphic event with top-to-the-SSE-SSW ductile shear in amphibolite facies affected the mantle rocks in the upper high-grade unit of the Kesebir dome (s.s.), both high-grade units in the Veykata and Byala reka domes, and the basement units in the Makaza dome. The subsequent deformational event that caused pervasive mylonitization of the footwall lower unit in the core of the Kesebir dome (s.s.) below the Tokachka detachment surface resulted in a consistently NNE-SSW–oriented stretching lineation associated with top-to-the-NNE ductile shearing (stereoplot *i,* Fig. 5; Bonev, 2002b; Bonev et al., 2006a). The progression of the deformation from ductile noncoaxial flow to semiductile and brittle deformation suggests a strain regime under constant direction and kinematic continuity from ductile to brittle field in both plastically behaved mylonites and cataclasites along and beneath the detachment. The NNE-directed ductile deformation occurred in a retrogressive fashion in decreasing temperatures and metamorphic conditions within a greenschist-facies field as indicated by the common existence of chlorite-white mica growth in shear bands of mylonites structurally below the brittle detachment (Fig. 8A). Transposition of the regional tectonic foliation (S_1) into isoclinal folds is associated with the development of an axial-planar cleavage (S_2; Fig. 8B) and occurs below the Tokachka detachment, where S_1 and S_2 foliation intensify, acquiring a mylonitic character (Sm) toward the brittle detachment. These relationships suggest that S_1 and Sm are closely related spatially and geometrically indistinguishable, controlling foliation patterns in the core of the dome. Small-scale, tight to isoclinal folds with strongly attenuated limbs and thickened hinges have axes oriented oblique to subparallel to the lineation (Fig. 6), showing pronounced north or east vergence. These are mostly drag folds, especially in migmatites, with axes rotated into parallelism toward the kinematic direction defined by stretching lineations during shearing. Development of a second planar fabric together with the greenschist-facies retrogression demonstrates that top-to-the-NNE shear fabrics relate to a distinct deformation event that is younger than the synmetamorphic, south-directed ductile shearing. The extensional deformation in the Kesebir dome (s.s) led to strong thinning of the upper high-grade unit, particularly pronounced in the northeastern closure of the dome, and to extensional exhumation of the lower high-grade unit in the footwall of the Tokachka detachment (Fig. 4).

These observations and relationships can be extended westward to the northern flank of the Veykata dome, where extension-related fabrics at the base of the detachment hangingwall are associated with development of a steeply NNE-dipping axial planar crenulation cleavage (S_2) in metapelitic rocks (Fig. 8C). This crenulation cleavage is parallel to the regional tectonic foliation (S_1). Away from the extensional mylonitic zone in the footwall of the detachment in the Kesebir dome (s.s.), top-to-the-NNE ductile shearing characterizes thin, discrete, and gently north-dipping mylonite zones. They have accommodated down-dip (normal) displacement toward the detachment surface in the core of the northern Makaza dome (section 2-2′, Fig. 4; Bonev, 2002a). There, however, the top-to-the-NNW to NNE ductile fabrics involved no retrogression into the greenschist facies during normal shear sense at deeper crustal levels (Fig. 8D). These observations in the Kesebir (s.s.) and Makaza domes suggest a continuum of ductile deformation in a north-north-eastward direction at separate structural levels (from deepest to shallow) within the footwall, in which deformation proceeded from amphibolite- to greenschist-facies conditions toward the detachment. A transitional, diffuse zone showing top-to-the-SSE-SSW contractional and NNE-directed extensional ductile fabrics related to both main deformation events is defined in the core of the Makaza dome (Fig. 5).

Top-to-the-SSW Extensional Fabrics

The Byala reka detachment is exposed in the central–eastern part of the Byala reka dome. The Byala reka detachment represents a regional-scale, low-angle (10°–25°) normal fault that separates, in the central part of the dome, a thin (~200 m) marble lid of the upper high-grade unit and the Paleocene–early Eocene sedimentary rocks in the hangingwall from the orthogneisses of the lower high-grade unit in its footwall. At the eastern periphery of the dome, the upper high-grade unit together with the overlying low-grade Mesozoic unit and the Eocene sedimentary rocks form the hangingwall, and the orthogneisses of the lower high-grade unit make the footwall. The detachment surface is underlain by a mylonitic shear zone that exhibits pervasive ductile to semiductile deformation fabrics and is overprinted by a brittle deformation at late stages. Cataclastic fault rocks such as breccia, cataclasite, and gouge define the brittle detachment surface, which constitutes the uppermost part of the shear zone. Cataclastic rocks have a matrix with a

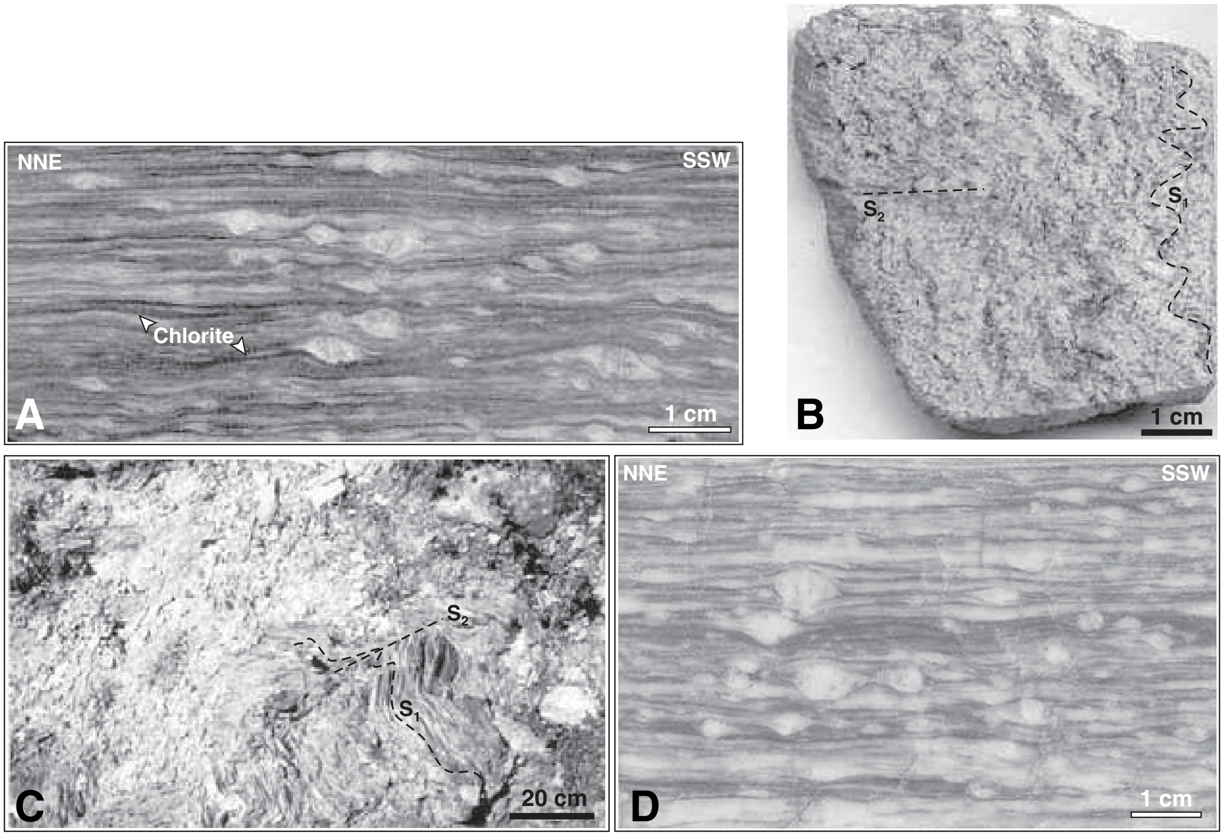

Figure 8. Ductile shear criteria and fabrics related with top-to-the-NNE extension. (A) Mylonitic augen gneiss in the shear zone structurally below the Tokachka detachment, polished sample. (B) Crenulation of regional foliation (S_1) with development of axial-planar cleavage (S_2), both parallel to mylonitic foliation (Sm) in shear zone. (C) Crenulation of regional foliation (S_1) in metapelite at the base of the Tokachka detachment hangingwall. (D) Mylonitic augen gneiss in a discrete shear zone, polished sample. See text for explanation; for locations, see Figure 5.

range of grain sizes, consisting of calcite, quartz, chlorite, and muscovite, which are similar in composition, as enclosed angular mineral fragments and clasts of marble and schist derived mainly from the upper high-grade unit. The common product of intense ductile deformation within the shear zone is mylonite, displaying a pervasive mylonitic foliation and stretching lineation. The mylonitic foliation (Sm) is flat-lying, striking NNW-SSE or north-south and dipping gently east-northeast (stereoplot *l,* Fig. 5). The mylonitic foliation contains a NNE-SSW–oriented stretching lineation with subhorizontal or shallow plunges in both directions (stereoplot *m,* Fig. 5) that is defined by elongated mineral grains, quartz-feldspar aggregates, and streaky phyllosilicates. Generally, the planar and linear fabrics in the shear zone parallel the brittle detachment surface and regional tectonic foliation (S_1) and lineation (L_1) in both the hangingwall and the footwall units (stereoplots *n* and *o,* Fig. 5). It is important to note that the stretching lineation within the shear zone can be distinguished by abundant chlorite crystallizations that distinguish the stretching lineation itself on both a micro- and an outcrop scale (Fig. 9A) from the regional lineation (L_1). Asymmetric, small-scale tight folds, mostly present in the hangingwall marbles, have axes consistently parallel to the lineation in the shear zone (Fig. 6).

Macro- and microsopic shear sense indicators are ubiquitous in the mylonites. They include winged K-feldspar σ-type porphyroclasts and garnet porphyroblasts, asymmetric extensional shear bands, and mica fishes (Fig. 9). Shear bands (the most common indicator) that include fine-grained chlorite and small recrystallized quartz grains transect the regional foliation (S_1). In mica-rich layers, individual mica flakes are reduced in grain size, forming abundant muscovite “fish” in between shear bands (Fig. 9B, C, and E). All these structures indicate strong noncoaxial flow with a consistent top-to-the-SSW shear sense (i.e., south-southwestward displacement of the hangingwall) along the low-angle detachment fault. Quartz shows evidence of strong internal deformation expressed by common undulose extinction, subgrains, and deformation bands indicative of intense dynamic recrystallization (mostly by means of subgrain rotation; Fig. 9B and E). Feldspar is deformed in a brittle fashion along syn- and antithetic fractures with respect to bulk flow di-

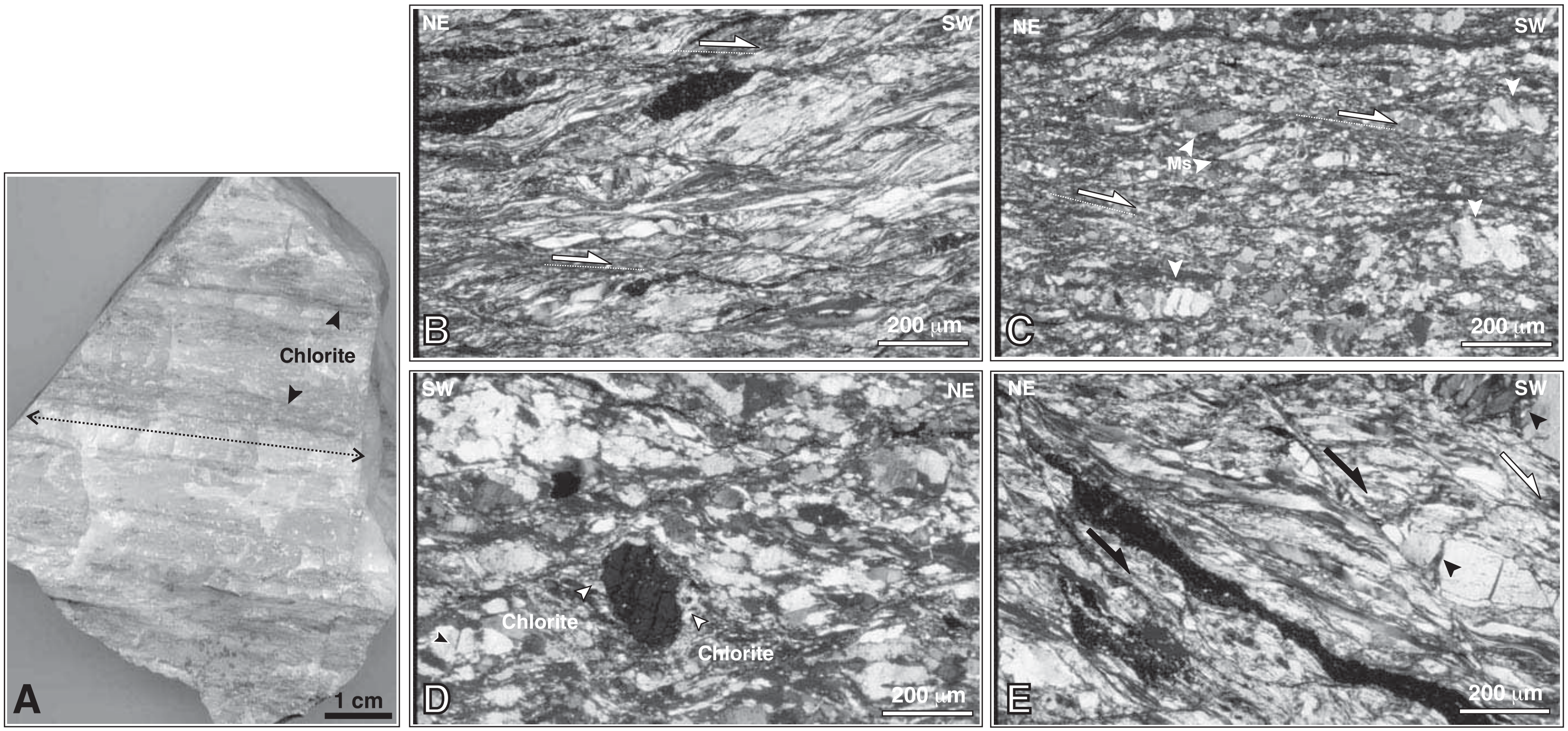

Figure 9. Ductile and brittle deformation structures and kinematic indicators associated with the top-to-the-SSW extension. (A) Stretching lineation defined by chlorite crystallizations (black arrows) in hand sample. (B) Top-to-the-southwest asymmetric extensional shear bands (white half-arrows) and mica "fish" in gneiss mylonite. Note the highly deformed and intensely recrystallized quartz in ribbons. (C) Muscovite fish (Ms), shear bands (large white half-arrows), and brittle fractured feldspar porphyroclasts (small white arrows) in gneiss mylonite. (D) Garnet porphyroblast with chlorite crystallized in asymmetric pressure shadows. Note also the brittle deformation of feldspar at lower left (black arrow) and the southwest-dipping shear bands. (E) Brittle shears (large black half-arrows) overprinting asymmetric extensional shear bands (large white half-arrow), both southwest-dipping. Small arrows indicate fractured feldspar. For locations, see Figure 5.

rection, resulting in irregularly shaped fragments (i.e., bookshelf arrangement; Fig. 9C). Fractures are usually filled with recrystallized quartz and feldspar fragments and become prominent in structurally upper levels of the shear zone toward the brittle low-angle fault. White mica and biotite are commonly bent in between adjacent shear bands due to slip along shear band cleavage.

Microstructural characteristics of quartz, feldspar, and micas associated with the mylonites constrain the temperatures of mylonitization in the shear zone during ductile to semiductile fabric formation to greenschist-facies conditions (i.e., 250–450 °C, e.g., Tullis and Yund, 1987; Pryer, 1993; Passchier and Trouw, 1996; Snoke et al., 1998). Retrogression after the main metamorphism in amphibolite facies is particularly well displayed by chlorite growth replacing biotite along the shear bands or forming pressure shadows around the pretectonic garnets with straight inclusion trails. These features indicate metamorphic reactions toward low pressures and temperatures under greenschist-facies conditions with respect to the contractional top-to-the-SSW shearing (Fig. 9D). The late-stage brittle deformation structures are represented by steeply SSW-dipping minor faults in outcrop scale and microshears reworking ductile to semiductile shear bands in a brittle manner with the same displacement direction (Fig. 9E).

On a large scale, the detachment surface is folded into open to closed short-wavelength kilometer-scale folds around northeast-southwest-trending subhorizontal to gently northeast-plunging fold axes. These larger-scale folds are observed in the marble lid in the central part of the dome as well as farther east along the Byala reka River, defined by the attitude of marbles and schists below the structurally overlying low-grade Mesozoic unit (Fig. 5). Antiformal structures are interpreted as detachment surface corrugation folds with axes parallel to the extension direction that are commonly associated with low-angle extensional faults (e.g., Mancktelow and Pavlis, 1994; Janecke et al., 1998).

The main argument for attributing top-to-the-SSW shearing to extension is based on the observation that shear zone mylonites in the lower high-grade unit of the footwall are directly overlain by cataclastic fault rocks found at the base of the hangingwall marble lid. In addition, cataclastic faulting at the base of the hangingwall and the upper structural levels of the shear zone also involves southwest-directed extension (Bonev et al., 2006a, and this study), implying kinematic continuity under decreasing metamorphic grade and temperatures of ductile then brittle deformation, which is also consistent with a low-angle extensional detachment.

TECTONIC MODEL AND KINEMATIC INTERPRETATION

Tectonic Model

Figure 10 summarizes structural and kinematic data regarding deformational events in a tectonic model for the Alpine collisional evolution of the high-grade metamorphic basement in the eastern Rhodope, also taking into account available sedimentary constraints and radiometric ages.

Structural and kinematic data and the deformation/crystallization relationships of the earliest deformational event relate this regionally coherent top-to-the-SSE-SSW–directed ductile shearing to contractional deformation during the synmetamorphic south-vergent thrusting and formation of the basement nappe stack. The temporal constraints of the contractional event are between ca. 119 and 65 Ma (see Table 1), including radiometric dates of peak metamorphism in eclogites and subsequent amphibolite-facies overprint (e.g., Mposkos and Wawrzenitz, 1995; Wawrzenitz and Mposkos, 1997; Liati et al., 2002). SSE-SSW-directed tectonic displacement accompanying high-pressure, high-temperature, and medium-pressure metamorphism developed during the northward subduction of the Vardar Ocean in an active margin setting followed by Alpine collision and crustal thickening (Fig. 10A). Ultra-high-pressure conditions at the initial stage of subduction were attained, but the age constraints remain controversial. Because imbrication of thrust slices in the high-grade basement units also involves oceanic crust material, this deformational event marks collision that is associated with peak metamorphism and south-vergent, foreland-directed thrusting consistent with the subduction polarity.

Structural analysis suggests that the top-to-the–SSW- and -NNE-directed event, variably overprinting previous contractional fabrics, is related to extension. This extensional event developed after peak metamorphism from amphibolite- to greenschist-facies in decreasing temperatures of ductile to brittle deformation conditions through the operation of extensional shear zones and low-angle detachments. This deformational event contributed to the unroofing of deep structural levels of the basement units and their extensional exhumation in metamorphic domes. Extension possibly commenced with the intrusion of late granites ca. 69–53 Ma (e.g., Ovtcharova et al., 2003; Marchev et al., 2004b), constraining at least a pre–latest Late Cretaceous age for the contractional tectonometamorphic event, which is also consistent with the sedimentary constraints provided by supradetachment deposits (discussed later). The timing of extension is bracketed by syntectonic hangingwall sedimentation, cooling ages of basement rocks in the detachment footwall, and hydrothermal alteration in the hangingwall rocks. Extension initiated with a low-dipping extensional shear zone formed at depth coupled with the low-angle detachments in the upper crustal level (Fig. 10B). The onset of extension is indicated by Paleocene sedimentary rocks deposited in half-grabens on the detachment hangingwall, implying that at that time a significant part of the upper high-grade unit was unroofed and substantially thinned by faulting in the hangingwall. Later, as extension proceeded, subsequent cooling and exhumation of the lower high-grade unit below detachments occurred ca. 42–37 Ma (e.g., Lips et al., 2000; Krohe and Mposkos, 2002; Bonev et al., 2006a), leading to updoming and the exhumation of gneissic cores in the footwall domes (Fig. 10). Late-stage

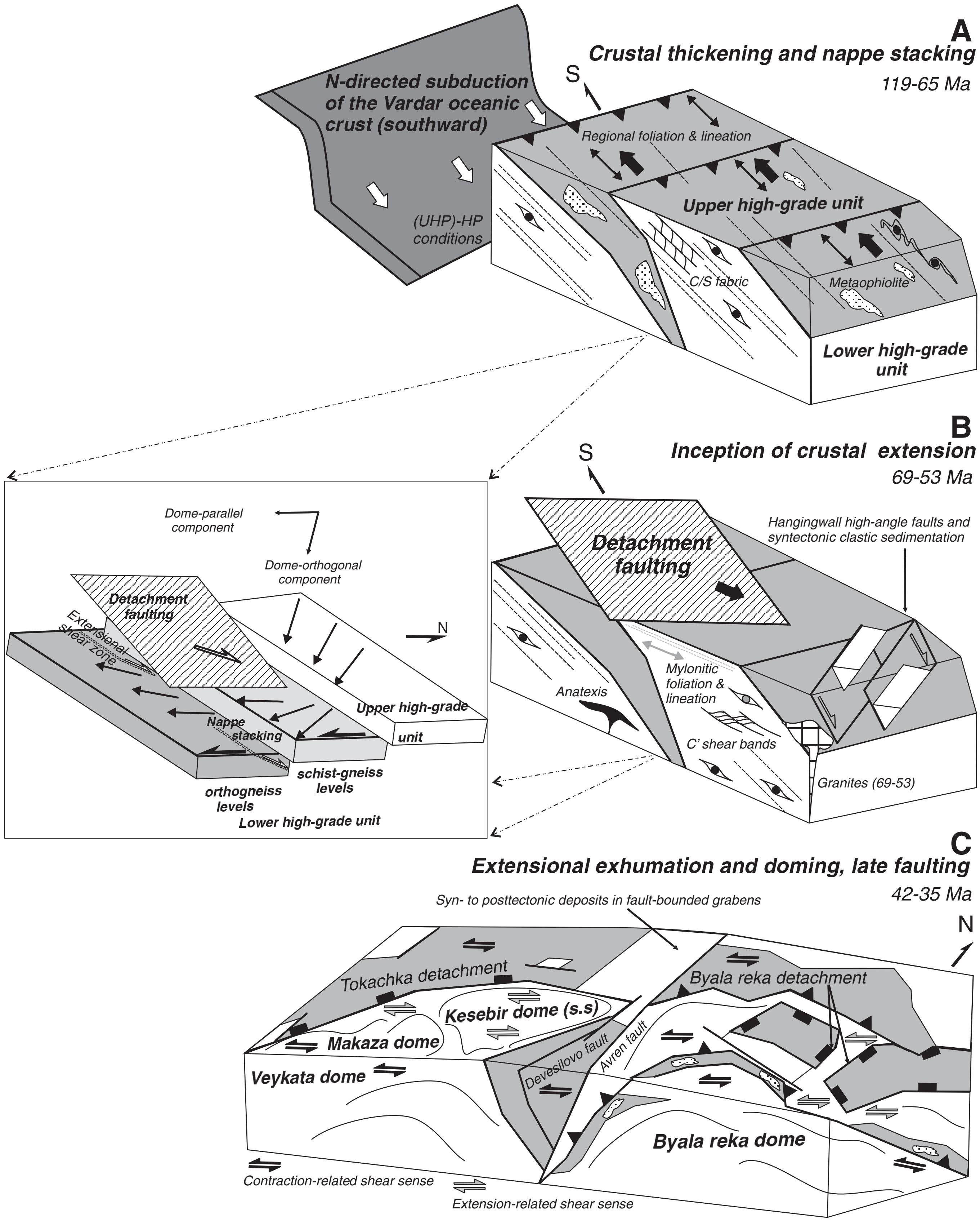

Figure 10. Schematic cartoon model proposed to account for the syn- to postcollisional evolution and kinematic direction variations in distinct units (inset) of the high-grade metamorphic basement.

upper-crustal brittle faulting accompanying extension took place between 36.5 and 35 Ma, as indicated by the ages of hydrothermal rocks along these faults in altered sedimentary packages of supradetachment deposits (Marchev et al., 2003, 2004a). Post-tectonic sedimentation of late Eocene–Oligocene age accompanied by volcanic activity persisted into the Oligocene, postdating the tectonic events.

Kinematic Interpretation

The mylonitic gneissic fabric and lithologies in the high-grade basement units overall exhibit a northwest-southeast to northeast-southwest lineation pattern that varies across the study area (Fig. 5). In the Veykata dome, the orientation of lineation changes significantly as a function of the structural level, in contrast to moderate changes of the foliation attitude. At deeper structural levels, the lineations are oriented northeast-southwest in the lower high-grade unit and trend northwest-southeast at higher structural levels in the upper high-grade unit. There, the swing of the lineation trend from a northeast to northwest direction with ascending structural level is complex, passing through contractional mylonite zones with orientations transitional between end-members. In the Makaza dome, the lineations exhibit an analogous pattern showing a NNW-SSE orientation in structurally upper levels and swing to a north-south or NNE-SSW trend at deeper structural levels within the core of the dome. Similarly, on the southeastern flank of the Kesebir dome (s.s.), lineations trend northeast-southwest and swing to northwest-southeast in the deepest structural levels of the upper high-grade unit, have a consistent northwest-southeast trend in the northwestern flank of the dome, and are oriented northeast-southwest in the core. The reorientation of lineations in the upper high-grade unit of the hangingwall occurs in the vicinity of the Tokachka detachment, most likely reflecting passive rotation into the bulk shear direction in the underlying ductile mylonites. Reorientation against late faults seems to be a local feature. Therefore, the trend of lineations is dependent on both structural level and proximity to the high-strain zones in either extensional or contractional mylonitic zones. Because stretching lineations are pervasively imprinted metamorphic tectonites throughout the study area, they mark the extension direction of bulk ductile flow, which is taken as a kinematic direction. This conclusion is also confirmed by finite strain analysis and quartz *c*-axis preferred orientations (Fig. 4; Bonev et al., 2006b).

To explain this lineation pattern, a model depicting variation across the large-scale Kesebir dome is proposed (inset, Fig. 10). The model evaluates the dependence of lineation pattern on both structural levels and tectonic contacts. In this model, the lineation pattern reflects vertically partitioned kinematic direction in the high-grade metamorphic units, including components of dome-orthogonal and dome-parallel slip that have resulted from thickening to extension-related deformations during the dome's evolution.

DISCUSSION

The close proximity of extensional metamorphic domes that record similar kinematic directions in their cores, but with opposite senses of extension, render necessary an explanation of the regional-scale picture of extensional tectonics. As a working hypothesis to address discrepancy, I propose that the Avren fault acted as a transfer fault with normal or strike-slip movement linking the Tokachka detachment and the Byala reka detachment faults in a conjugate system. The Avren fault has accommodated displacement in domains with opposite-sense ductile flow at deeper levels in the footwall of both domes. The fault presents evidence for normal displacement along the map trace as well as a less obvious strike-slip component of movement. In Greece, the pattern of faults that controlled the formation of late Eocene–Oligocene to Miocene sedimentary basins has been interpreted as large-scale dextral slip shear related to either oblique convergence or activity on the North Anatolian fault. The late Eocene–Oligocene extensional collapse basins were cut by strike-slip faulting on normal and dominantly dextral strike-slip faults, which began in Oligocene times (Karfakis and Doutsos, 1995) and persisted into the Miocene–present (Koukouvelas and Aydin, 2002). The regional fault pattern and kinematics, distribution of sedimentary basins and their fill (e.g., Fig. 2), and seismic data (Velev, 1996) suggest that the late Eocene–Oligocene Avren fault normal or strike-slip system was active at the same time that the cooling and exhumation of metamorphic domes and the latest brittle extension (ca. 37–35 Ma) was occurring.

The following points and criteria are considered vital in the interpretation of ductile fabrics and kinematics created during deformation events in the high-grade metamorphic basement:

1. Ductile deformation fabrics show evidence of separate events. Separation of the structures formed during distinct phases or events is greatly hampered, and the sequence of events can be established only locally because they developed broadly under the same amphibolite-facies conditions with little or no retrogression involved. Different fabrics often share the same foliation orientation, and this foliation has been locally transposed. However, the greenschist-facies retrogression of pervasive ductile fabrics and kinematics allows distinguishing dominant ductile deformation events in the vicinity of detachments.
2. Top-to-the-SSE-SSW ductile shear coeval with amphibolite-facies metamorphism caused pre-dome penetrative fabric development and synmetamorphic nappe stacking in the basement rocks involving oceanic crust.
3. Top-to-the-SSW ductile shear outlasted the nappe-stacking event and featured with the same sense of tectonic transport during extension. The extensional deformation was associated with the retrogression of mineral assemblages delineating previous fabrics under lower greenschist-facies meta-

morphism. This feature is best exemplified in the Byala reka dome.

4. Top-to-the-NNE ductile extensional shear in the core of the Kesebir dome (s.s.) can be easily distinguished from contractional structures. In the case of the Makaza dome, transitional character between the fabrics and kinematics of both events is displayed, which passes into the entirely contraction-related fabrics and kinematics in the Veykata dome. This suggests broadly contemporaneous deep- to midlevel crustal stacking and extension.

Summarizing, the tectonic pattern of the high-grade basement in the eastern Rhodope relates to the tectonic processes of subduction-collision in an active orogenic wedge during the Mid–Late Cretaceous to Tertiary time. Collision resulted in foreland-directed basement nappe stacking and associated ductile deformation and metamorphism in pre-latest Late Cretaceous time. Following crustal thickening and cessation of the Alpine convergence, the Early to Mid-Tertiary crustal extension has governed both foreland- and hinterland-directed unroofing of the original nappe stack through the operation of low-angle detachments and extensional shear zones. The Cenozoic tectonic evolution of the eastern Rhodope sketches the importance of syn- to postcollisional processes in modeling the structural shape of the Alpine orogen in this part of the eastern Mediterranean region.

CONCLUSIONS

This preliminary synthesis of the tectonic pattern of the eastern Rhodope highlights the following main features of high-grade basement structure and kinematics:

1. The metamorphic basement presents large-scale Alpine extensional metamorphic domes, namely the Byala reka dome and the Kesebir dome, that were exhumed in the footwalls of low-angle detachments. These prominent large-scale structures record ductile flow related to crustal stacking and extension-related episodes during Alpine collisional evolution.
2. Two kinematically distinct contractional and extensional deformation events are imprinted with pervasive ductile fabrics in the metamorphic pile: top-to-the-SSE-SSW crustal stacking coeval with dominant metamorphism in amphibolite facies, followed by top-to-the–SSW- and top-to-the-NNE-directed ductile to brittle extension during upper greenschist-facies conditions of deformation.
3. The crustal extension that dominates the large-scale tectonic pattern in the eastern Rhodope links the region as an important extensional domain in the late Alpine Aegean extensional province. Syn- to postcollisional tectonic processes played a key role in the structural modeling of that domain during the late orogenic evolution.

ACKNOWLEDGMENTS

The author is grateful for the support provided by Sofia University "St. Kliment Ohridski" and the University of Lausanne during the past few years, which helped him with field and laboratory work. Critical reviews by John Wakabayachi and Ron Harris are gratefully acknowledged. Review, thorough editorial comments, and valuable suggestions from Yildirim Dilek helped to improve the manuscript and are gratefully acknowledged.

REFERENCES CITED

Barr, S.R., Temperley, S., and Tarney, J., 1999, Lateral growth of the continental crust through deep level subduction-accretion: A re-evaluation of central Greek Rhodope: Lithos, v. 46, p. 69–94, doi: 10.1016/S0024-4937(98)00055-3.

Biggazzi, G., Del Moro, A., Innocenti, F., Kiryakopoulos, K., Manetti, P., Papadopoulos, P., Norelitti, P., and Magganas, A., 1989, The magmatic intrusive complex of Petrota, west Thrace: Age and geodynamic significance: Geologica Rhodopica, v. 1, p. 290–297.

Bonchev, E., 1971, Problems of the Bulgarian geotectonics: Sofia, Technika, 204 p.

Bonev, N., 1996, Tokachka shear zone southwest of Krumovgrad in the Eastern Rhodopes, Bulgaria: An extensional detachment: Annuaire de l'Université de Sofia, Faculté de Géologie et Géographie, Livre 1 Géologie, v. 89, p. 97–106.

Bonev, N., 1999, Extensional exhumation of metamorphic complexes in the Kesebir gneiss dome, Eastern Rhodope (South Bulgaria): EOS (Transactions, American Geophysical Union), v. 80, no. 46, p. 1066.

Bonev, N.G., 2001, Extension of syn-metamorphic thrust system in a part of Eastern Rhodope in the area north of Veykata summit, South Bulgaria: Comptes Rendus de l'Académie bulgare des Sciences, v. 54, p. 61–66.

Bonev, N.G., 2002a, Ductile NW-SE fabric and shear sense variations on a cross-section along Makaza pass, Eastern Rhodope, South Bulgaria: Structural and kinematic data: Comptes Rendus de l'Académie bulgare des Sciences, v. 55, p. 83–88.

Bonev, N., 2002b, Structure and evolution of the Kesebir gneiss dome, Eastern Rhodope [Ph.D. thesis]: University of Sofia, Sofia, 282 p.

Bonev, N.G., 2004, Sillimanite-bearing migmatites from the Rhodope metamorphic complexes, southern Bulgaria: Occurrence and implications for the tectono-metamorphic history: Neues Jahrbuch für Geologie und Paläontologie Abhandlungen, v. 232, p. 57–75.

Bonev, N., 2006, Structural and geochemical studies on amphibolite and greenschist-facies rocks in the Kulidjik River valley, eastern Rhodope, Bulgaria: Preliminary results: Neues Jahrbuch für Geologie und Paläontologie Abhandlungen, v. 239, p. 161–181.

Bonev, N.G., and Stampfli, G.M., 2003, New structural and petrologic data on Mesozoic schists in the Rhodope (Bulgaria): Geodynamic implications: Comptes Rendus Geoscience, v. 335, p. 691–699, doi: 10.1016/S1631-0713(03)00122-6.

Bonev, N., Marchev, P., and Singer, B., 2006a, Au, $^{40}Ar/^{39}Ar$ geochronology constraints on the Middle Tertiary basement extensional exhumation, and its relation to ore-forming and magmatic processes in the Eastern Rhodope (Bulgaria): Geodinamica Acta, v. 19, in press.

Bonev, N., Burg, J.-P., and Ivanov, Z., 2006b, Mesozoic–Tertiary structural evolution of an extensional gneiss dome: The Kesebir-Kardamos Dome, Eastern Rhodope (Bulgaria-Greece): International Journal of Earth Sciences, v. 95, p. 318–340, doi: 10.1007/s00531-005-0025-y.

Boyanov, I., 1969, Notes on the Kulidjik nappe: Bulletin of the Geological Institute of the Bulgarian Academy of Sciences, series Geotectonics, v. 18, p. 159–165.

Boyanov, I., and Goranov, A., 2001, Late Alpine (Palaeogene) superimposed depressions in parts of Southeast Bulgaria: Geologica Balcanica, v. 31, p. 3–36.

Boyanov, I., and Kozhoukharov, D., 1968, Structure and block subdivision of the Rhodope massif: Bulletin of the Geological Institute of the Bulgarian Academy of Sciences, series Geotectonics: Stratigraphy and Lithology, v. 17, p. 199–226.

Boyanov, I., and Russeva, M., 1989, Lithostratigraphy and tectonic position of the Mesozoic rocks in the East Rhodopes: Geologica Rhodopica, v. 1, p. 22–33.

Boyanov, I., Mavrudchiev, B., and Vaptzarov, I., 1963, On the structural and formation features in part of East Rhodopes: Bulletin of the Geological Institute of the Bulgarian Academy of Sciences, v. 12, p. 125–186.

Burchfiel, B.C., 1980, Eastern European Alpine system and the Carpathian orocline as an example of collision tectonics: Tectonophysics, v. 63, p. 31–61, doi: 10.1016/0040-1951(80)90106-7.

Burchfiel, B.C., Nakov, R., and Tzankov, T., 2003, Evidence from the Mesta half-graben, SW Bulgaria, for the Late Eocene beginning of Aegean extension in the central Balkan Peninsula: Tectonophysics, v. 375, p. 61–76, doi: 10.1016/j.tecto.2003.09.001.

Burg, J.-P., Ivanov, Z., Ricou, L.-E., Dimor, D., and Klain, L., 1990, Implications of shear-sense criteria for the tectonic evolution of the Central Rhodope Massif, southern Bulgaria: Geology, v. 18, p. 451–454, doi: 10.1130/0091-7613(1990)018<0451:IOSSCF>2.3.CO;2.

Burg, J.-P., Ricou, L.-E., Ivanov, Z., Godfriaux, I., Dimov, D., and Klain, L., 1996, Syn-metamorphic nappe complex in the Rhodope Massif: Structure and kinematics: Terra Nova, v. 8, p. 6–15.

Carrigan, C., Mukasa, S., Haydoutov, I., and Kolcheva, K., 2003, Ion microprobe U-Pb zircon ages of pre-Alpine rocks in the Balkan, Sredna Gora and Rhodope terranes of Bulgaria: Constraints on Neoproterozoic and Variscan evolution: Journal of the Czech Geological Society, v. 48, p. 32–33.

Del Moro, A., Innocenti, F., Kyriakopoulos, K., Manetti, P., and Papadopoulos, P., 1988, Tertiary granitoids from Thrace (northern Greece): Sr isotopic and petrochemical data: Neues Jahrbuch für Mineralogie-Abhandlungen, v. 159, p. 113–135.

Dercourt, J., Zonenshain, L.P., Ricou, L.-E., Kazmin, V.G., Le Pichon, X., Knipper, A.L., Grandjacquet, C., Sbortshhikov, I.M., Geyssant, J., Lepvrier, C., Perchersky, D.H., Boulin, J., Sibuet, J.-C., Savostin, L.A., Sorokhtin, O., Wesphal, M., Bazhrnov, M.L., Lauer, J.-P., and Biju-Duval, B., 1986, Geological evolution of the Tethys belt from the Atlantic to the Pamirs since the Lias: Tectonophysics, v. 123, p. 241–315, doi: 10.1016/0040-1951(86)90199-X.

Dewey, J.F., and Şengör, A.M.C., 1979, Aegean and surrounding regions: Complex multiplate and continuum tectonics in a convergent zone: Geological Society of America Bulletin, v. 90, p. 84–92, doi: 10.1130/0016-7606(1979)90<84:AASRCM>2.0.CO;2.

Dimadis, E., and Nikolov, T., 1997, An ammonite find in the Makri unit (Berriasian, southeast Rhodopes, northeast Greece): Comptes Rendus de l'Académie bulgare des Sciences, v. 50, p. 71–74.

Dinter, D.A., 1998, Late Cenozoic extension of the Alpine collisional orogen, northeastern Greece: Origin of the north Aegean basin: Geological Society of America Bulletin, v. 110, p. 1208–1230, doi: 10.1130/0016-7606(1998)110<1208:LCEOTA>2.3.CO;2.

Dinter, D.A., and Royden, L., 1993, Late Cenozoic extension in northeastern Greece: Strymon valley detachment system and Rhodope metamorphic core complex: Geology, v. 21, p. 45–48, doi: 10.1130/0091-7613(1993)021<0045:LCEING>2.3.CO;2.

Dinter, D.A., Macfarlane, A.M., Hames, W., Isachsen, C., Bowring, S., and Royden, L., 1995, U-Pb and $^{40}Ar/^{39}Ar$ geochronology of the Symvolon granodiorite: Implications for the thermal and structural evolution of the Rhodope metamorphic core complex, northeastern Greece: Tectonics, v. 14, p. 886–908, doi: 10.1029/95TC00926.

Dutruge, G., 1996, Analyse petrostructurale de la localization de la déformation ductile dans les zones de cisaillement [Ph.D. thesis]: Université Montpellier II, Montpellier, 234 p.

Goranov, A., and Atanasov, G., 1992, Lithostratigraphy and formation conditions of Maastrichtian–Paleocene deposits in Krumovgrad District: Geologica Balcanica, v. 22, p. 71–82.

Goranov, A., Kozhoukharov, D., Boyanov, I., and Kozhoukharova, E., 1995, Geological map of Bulgaria, Committee of Geology Map Sheet Krumovgard and Sape, 1 sheet, 97 p. text, scale 1:100 000.

Harkovska, A., Yanev, Y., and Marchev, P., 1989, General features of the Paleogene orogenic magmatism in Bulgaria: Geologica Balcanica, v. 19, p. 37–72.

Haydoutov, I., Kolcheva, K., Daieva, L., and Savov, I., 2001, Island-arc origin of the Neoproterozoic variegated formations from the East Rhodopes (Avren synform and Bela Reka antiform), Bulgaria: European Science Foundation Europrobe meeting, Ankara: Abstracts, v. 1, p. 31–32.

Innocenti, F., Kolios, N., Manetti, P., Mazzuoli, R., Peccerillo, A., Rita, F., and Villari, L., 1984, Evolution and geodynamic significance of Tertiary orogenic volcanism in northeastern Greece: Bulletin of Vulcanology, v. 47, p. 25–37, doi: 10.1007/BF01960538.

Ivanov, R., 1961, Stratigraphy and structure of the crystalline in the Eastern Rhodope: Works on the geology of Bulgaria, series Geochemistry and Ore Deposits: Bulgarian Academy of Sciences, v. 2, p. 69–119.

Ivanov, R., 1981, The deep-seated Central Rhodope nappe and the interference tectonics of the Rhodope crystalline basement: Geologica Balcanica, v. 11, p. 47–66.

Ivanov, Z., 1988, Aperçu général sur l'évolution géologique et structurale du massif des Rhodopes dans le cadre des Balkanides: Bulletin de la Société Géologique de France, v. 8, no. 4, p. 227–240.

Ivanov, R., and Kopp, K.O., 1969, Das Alttertiär Thrakiens und der Ostrhodope: Geologica et Paleontologica, v. 3, p. 123–153.

Ivanov, Z., Moskovski, S., Dimov, D., Kolcheva, K., and Klain, L., 1985, Geological structure of the Central Rhodopes, II: Structural sequences in the syn-metamorphic evolution of the Central Rhodope Metamorphic Group: Geologica Balcanica, v. 15, p. 3–32.

Jacobshagen, V., Durr, S., Kockel, F., Kopp, K.O., Kowalczyk, G., Berckhamer, H., and Buttner, D., 1978, Structure and geodynamic evolution of the Aegean region, *in* Cloos, H., et al., eds., Alps, Appenines, Hellenides: Stuttgart, E. Schweizerbart, p. 537–564.

Janecke, S.U., Vandenburg, C.J., and Blankenau, J.J., 1998, Geometry, mechanisms and significance of extensional folds from examples in the Rocky Mountain Basin and Range province, U.S.A: Journal of Structural Geology, v. 20, p. 841–856, doi: 10.1016/S0191-8141(98)00016-9.

Jaranov, D., 1960, Tectonics of Bulgaria: Sofia, Technika, 282 p.

Karfakis, I., and Doutsos, T., 1995, Late orogenic evolution of the Circum-Rhodope belt, Greece: Neues Jahrbuch für Geologie und Paläontologie Monatshefte, v. H5, p. 305–319.

Kauffmann, G., Kockel, F., and Mollat, H., 1976, Notes on the stratigraphic and paleogeographic position of the Svoula Formation in the innermost zones of the Hellenides (Northern Greece): Bulletin de la Société Géologique de France, v. 7, no. 18, p. 225–230.

Kilias, A., and Mountrakis, D., 1990, Kinematics of the crystalline sequences in the Western Rhodope massif: Geologica Rhodopica, v. 2, p. 100–116.

Kilias, A.A., and Mountrakis, D.M., 1998, Tertiary extension of the Rhodope massif associated with granite emplacement (Northern Greece): Acta Vulcanologica, v. 10, p. 331–337.

Kilias, A., Falalakis, G., and Mountrakis, D., 1999, Cretaceous–Tertiary structures and kinematics of the Serbomacedonian metamorphic rocks and their relation to the exhumation of the Hellenic hinterland (Macedonia, Greece): International Journal of Earth Sciences, v. 88, p. 513–531, doi: 10.1007/s005310050282.

Kober, L., 1928, Der Bau der Erde: Berlin, Borntraeger, 499 p.

Kockel, F., Mollat, H., and Walther, H.W., 1977, Erläuterungen zur geologicschen Karte der Chalkidiki und angrenzender Gebiete 1/100.000 (Nord

Griechenland): Hanover, Bundesanstalt für Geowissenschaften und Rohstoffe, 119 p.

Kolcheva, K., and Eskenazy, G., 1988, Geochemistry of metaeclogites from the Central and Eastern Rhodope Mountains: Geologica Balcanica, v. 18, p. 61–78.

Koukouvelas, I., and Aydin, A., 2002, Fault structure and related basins of the North Aegean Sea: Tectonics, v. 21, p. 1–17, doi: 10.1029/2001TC901037.

Koukouvelas, I., and Doutsos, T., 1990, Tectonic stages along a traverse cross cutting the Rhodopian zone (Greece): Geologische Rundschau, v. 79, p. 753–776, doi: 10.1007/BF01879213.

Kozhoukharov, D., 1971, East Rhodope block: Structural complexes and structural plans, *in* Yovchev, Y., ed., Tectonic structure of Bulgaria: Sofia, Technika, p. 100–127.

Kozhoukharov, D., Kozhoukharova, E., and Papanikolau, D., 1988, Precambrian in the Rhodope massif, *in* Zoubek, V., et al., eds., Precambrian in younger fold belts—European Variscides, the Carpathians and Balkans: Chichester, John Wiley and Sons, p. 723–778.

Kozhoukharova, E., 1984, Origin and structural position of the serpentinized ultrabasic rocks of the Precambrian ophiolitic association in the Rhodope Massif, I: Geologic position and composition of ophiolite association: Geologica Balcanica, v. 14, p. 9–36.

Kozhoukharova, E., 1998, Eclogitization of serpentinites into narrow shear zones from the Avren syncline, Eastern Rhodopes: Geochemistry, Mineralogy and Petrology, v. 35, p. 29–46.

Krohe, A., and Mposkos, E., 2002, Multiple generations of extensional detachments in the Rhodope Mountains (northern Greece): Evidence of episodic exhumation of high-pressure rocks, *in* Blundell, D.J., et al., eds., The timing and location of major ore deposits in an evolving orogen: Geological Society of London Special Publication 204, p. 151–178.

Liati, A., 1988, Amphibolized eclogites in the Rhodope crystalline complex, near Xanthi (N. Greece): Neues Jahrbuch für Mineralogie Monatshefte, v. H1, p. 1–8.

Liati, A., and Mposkos, E., 1990, Evolution of eclogites in the Rhodope zone of northern Greece: Lithos, v. 25, p. 89–99, doi: 10.1016/0024-4937(90)90008-O.

Liati, A., and Siedel, E., 1996, Metamorphic evolution and geochemistry of kyanite eclogites in central Rhodope, northern Greece: Contributions to Mineralogy and Petrology, v. 123, p. 293–307, doi: 10.1007/s004100050157.

Liati, A., Gebauer, D., and Wysoczanski, R., 2002, U-Pb SHRIMP-dating of zircon domains from UHP garnet-rich mafic rocks and late pegmatoids in the Rhodope zone (N Greece): Evidence for Early Cretaceous crystallization and Late Cretaceous metamorphism: Chemical Geology, v. 184, p. 281–299, doi: 10.1016/S0009-2541(01)00367-9.

Lips, A.L.W., White, S.H., and Wijbrans, J.R., 2000, Middle–Late Alpine thermotectonic evolution of the southern Rhodope Massif, Greece: Geodinamica Acta, v. 13, p. 281–292, doi: 10.1016/S0985-3111(00)00042-5.

Macheva, L.A., 1998, 3T-phengites in the rocks of Biala reka metamorphic group: An indicator for high-pressure metamorphism: Geochemistry, Mineralogy and Petrology, v. 35, p. 17–28.

Macheva, L., and Kolcheva, K., 1992, Metagranitoids from east Rhodopes: Occurrence and main features: Comptes Rendus de l'Académie bulgare des Sciences, v. 45, p. 63–66.

Mancktelow, N.S., and Pavlis, T.L., 1994, Fold-fault relationships in low-angle detachment systems: Tectonics, v. 13, p. 668–685, doi: 10.1029/93TC03489.

Marchev, P., Singer, B., Andrew, C., Hasson, S., Moritz, R., and Bonev, N., 2003, Characteristics and preliminary $^{40}Ar/^{39}Ar$ and $^{87}Sr/^{86}Sr$ data of the Upper Eocene sedimentary-hosted low-sulfidation gold deposits Ada Tepe and Rosino, SE Bulgaria: Possible relation with core complex formation, *in* Eliopoulos D.G. et al., eds., Mineral exploration and sustainable development: Rotterdam, Millpress, v. 2, p. 1193–1196.

Marchev, P., Singer, S.B., Jelev, D., Hasson, S., Moritz, R., and Bonev, N., 2004a, The Ada Tepe deposit: A sediment-hosted, detachment fault-controlled, low-sulfidation gold deposit in the Eastern Rhodopes, SE Bulgaria: Schweizerische Mineralogische und Petrographische Mitteilungen, v. 84, nos. 1-2, p. 59–78.

Marchev, P., Raicheva, R., Downes, H., Vaselli, O., Chiaradia, M., and Moritz, R., 2004b, Compositional diversity of Eocene–Oligocene basaltic magmatism in the Eastern Rhodopes, SE Bulgaria: Implications for genesis and tectonic setting: Tectonophysics, v. 393, p. 301–328, doi: 10.1016/j.tecto.2004.07.045.

Meyer, W., 1968, Alterstellung des Plutonismus im Südteil der Rila-Rhodope-Masse: Geologica et Paleontologica, v. 2, p. 177–192.

Meyer, W., 1969, Die Faltenachsen im Rhodopen-Kristallin östlich des Strimon (Nordost-Griecheenland): Geotektonische Forschung, v. 31, p. 86–96.

Mposkos, E., 1989, High-pressure metamorphism in gneisses and pelitic schists in the East Rhodope Zone (N. Greece): Mineralogy and Petrology, v. 41, p. 25–39, doi: 10.1007/BF01164808.

Mposkos, E., 1998, Cretaceous and Tertiary tectonometamorphic events in Rhodope zone (Greece): Petrological and geochronological evidences: Bulletin of the Geological Society of Greece, v. 32, p. 59–67.

Mposkos, E., 2002, Petrology of the ultra-high pressure metamorphic Kimi complex in Rhodope (N.E. Greece): A new insight into the Alpine geodynamic evolution of the Rhodope: Bulletin of the Geological Society of Greece, v. 34, p. 2169–2188.

Mposkos, E., and Krohe, A., 2000, Petrological and structural evolution of continental high-pressure (HP) metamorphic rocks in the Alpine Rhodope Domain, *in* Panaydes, I., et al., eds., Proceedings of the 3rd International Conference on the Geology of the Eastern Mediterranean: Nicosia, Cyprus, Geological Survey Department, p. 221–232.

Mposkos, E.D., and Kostopoulos, D.K., 2001, Diamond, former coesite and supersilicic garnet in metasedimentary rocks from the Greek Rhodope: A new ultrahigh-pressure metamorphic province established: Earth and Planetary Science Letters, v. 192, p. 497–506, doi: 10.1016/S0012-821X(01)00478-2.

Mposkos, E., and Liati, A., 1993, Metamorphic evolution of metapelites in the high-pressure terrane of the Rhodope zone, northern Greece: Canadian Mineralogist, v. 31, p. 401–424.

Mposkos, E., and Wawrzenitz, N., 1995, Metapegmatites and pegmatites bracketing the time of HP-metamorphism in polymetamorphic rocks of the E. Rhodope, northern Greece: Petrological and geochronological constraints: Geological Society of Greece Special Publication 4, p. 602–608.

Mukasa, S., Haydoutov, I., Carrigan, C., and Kolcheva, K., 2003, Thermobarometry and $^{40}Ar/^{39}Ar$ ages of eclogitic and gneissic rocks in the Sredna Gora and Rhodope terranes of Bulgaria: Journal of the Czech Geological Society, v. 48, p. 94–95.

Ovtcharova, M., Quadt, A.V., Heinrich, C.A., Frank, M., Kaiser-Rohmeier, M., Peytcheva, I., and Cherneva, Z., 2003, Triggering of hydrothermal ore mineralization in the Central Rhodopean Core Complex (Bulgaria): Insight from isotope and geochronological studies on tertiary magmatism and migmatisation, *in* Eliopoulos, D.G., et al., eds., Mineral exploration and sustainable development, v. 1: Rotterdam, Millpress, p. 367–370.

Papanikolaou, D., and Panagopoulos, A., 1981, On the structural style of southern Rhodope, Greece: Geologica Balcanica, v. 11, p. 13–22.

Papanikolau, D., 1997, The tectonostratigraphic terranes of the Hellenides: Annales géologiques des Pays Helléniques, v. 37, p. 495–514.

Passchier, C.W., and Trouw, R.A.J., 1996, Micro-tectonics: Berlin, Springer, 289 p.

Peytcheva, I., and Quadt, A.V., 1995, U-Pb zircon dating of metagranites from Byala Reka region in the east Rhodopes, Bulgaria: Geological Society of Greece Special Publication 4, p. 637–642.

Peytcheva, I., Ovtcharova, M., Sarov, S., and Kostitsin, J., 1998, Age and metamorphic evolution of metagranitoids from Kesebir reka region, Eastern Rhodopes: Rb-Sr isotope data: XVI Congress of the Carpatho-Balkan Geological Association, Vienna, Abstracts, p. 471.

Peytcheva, I., Kostitsin, Y., Salnikova, E., von Quadt, A., Kamenov, B., and Klain, L., 1999, Alpine evolution of the magmatism in the West-Rhodopes: Rb-Sr and U-Pb isotope data: Journal of Conference Abstracts, v. 4, p. 470.

Pryer, L.L., 1993, Microstructures in feldspar from a major crustal thrust zone: The Grenville front, Ontario, Canada: Journal of Structural Geology, v. 15, p. 21–36.

Ricou, L.-E., Burg, J.-P., Godfriaux, I., and Ivanov, Z., 1998, Rhodope and Vardar: The metamorphic and the olistostromic paired belts related to the Cretaceous subduction under Europe: Geodinamica Acta, v. 11, p. 285–309, doi: 10.1016/S0985-3111(99)80018-7.

Robertson, A.H.F., and Dixon, J.E., 1984, Introduction: Aspects of the geological evolution of the Eastern Mediterranean, *in* Dixon, J.E., and Robertson, A.H.F., eds., The geological evolution of the Eastern Mediterranean: Geological Society of London Special Publication 17, p. 1–74.

Robertson, A.H.F., Dixon, J.E., Brown, S., Collins, A., Morris, A., Pickett, E., Sharp, I., and Ustaömer, T., 1996, Alternative tectonic models for the Late Palaeozoic–Early Tertiary development of Tethys in the Eastern Mediterranean region, *in* Morris, A., and Tarling, D.H., eds., Paleomagnetism and tectonics of the Mediterranean region: Geological Society of London Special Publication 105, p. 239–263.

Snoke, A.W., Tullis, J., and Todd, V.R., 1998, Fault-related rocks: A photographic atlas: Princeton, New Jersey, Princeton University Press, 617 p.

Sokoutis, D., Brun, J.-P., Van Den Driessche, J., and Pavlides, S., 1993, A major Oligo-Miocene detachment in southern Rhodope controlling north Aegean extension: Journal of the Geological Society of London, v. 150, p. 243–246.

Soldatos, T., and Christofides, G., 1986, Rb-Sr geochronology and origin of the Elatia Pluton, Central Rhodope, North Greece: Geologica Balcanica, v. 16, p. 15–23.

Tikhomirova, L.B., Boyanov, I., and Zagorchev, I., 1988, Early Jurassic radiolarians from the Eastern Rhodopes: A revision of the age of Dolno Lukovo Formation: Geologica Balcanica, v. 18, p. 58.

Trikkalinos, J.K., 1955, Beiträge zur Erforschung des tektonischen Baues Griechenlands: Über das Alter der vortertiären Schichten des Gebietes von Alexandroupolis-Didymotichon-Westthrazien: Annales géologiques des Pays Helléniques, v. 1, p. 81–82.

Tsikouras, B., Pe-Piper, G., and Hatzipanagiotou, K., 1990, A new date of an ophiolite on the northeastern margin of the Vardar Zone, Samothraki, Greece: Neues Jahrbuch für Mineralogie Monatshefte, v. 11, p. 521–527.

Tullis, J., and Yund, R.A., 1987, Transition from cataclastic flow to dislocation creep in feldspar: Mechanism and microstructure: Geology, v. 15, p. 606–609, doi: 10.1130/0091-7613(1987)15<606:TFCFTD>2.0.CO;2.

Velev, A., 1996, Deep seismic section of the crust on regional profile Ardino-Ivaylovgrad: Review of Bulgarian Geophysics, v. 22, p. 91–109.

Wawrzenitz, N., and Krohe, A., 1998, Exhumation and doming of the Thasos metamorphic core complex (S. Rhodope, Greece): Structural and geochronological constraints: Tectonophysics, v. 285, p. 301–332, doi: 10.1016/S0040-1951(97)00276-X.

Wawrzenitz, N., and Mposkos, E., 1997, First evidence for Lower Cretaceous HP/HT-metamorphism in the Eastern Rhodope, North Aegean Region, North-East Greece: European Journal of Mineralogy, v. 9, p. 659–664.

Yanev, Y., and Bardintzeff, J.-M., 1997, Petrology, volcanology and metallogeny of Palaeogene collision-related volcanism of the Eastern Rhodopes (Bulgaria): Terra Nova, v. 9, p. 1–8, doi: 10.1046/j.1365-3121.1997.d01-3.x.

Manuscript Accepted by the Society 30 December 2005

Geological Society of America Special Papers

Cenozoic tectonic evolution of the eastern Rhodope massif (Bulgaria): Basement structure and kinematics of syn- to postcollisional extensional deformation

Nikolay Bonev

Geological Society of America Special Papers 2006;409; 211-235
doi:10.1130/2006.2409(12)

Notes